Volume I

FALLOUT AND RADIOLOGICAL COUNTERMEASURES

Prepared for:

OFFICE OF CIVIL DEFENSE
DEPARTMENT OF DEFENSE
WASHINGTON, D.C.

STANFORD RESEARCH INSTITUTE

MENLO PARK, CALIFORNIA

Table 2.3

CUMULATIVE MASS-CHAIN YIELDS OF FISSION PRODUCTS
(VALUES ARE IN PERCENT OF FISSIONS)

Mass Number	U-235		U-238		Pu-239	
	Thermal Neutrons*	Fission Neutrons	Fission Neutrons	8-Mev Neutrons	Thermal Neutrons	Fission Neutrons
72	1.6×10^{-5}	4.6×10^{-4}	5.0×10^{-6}	-	1.2×10^{-4}*	-
73	1.1×10^{-4}	0.0012	3.7×10^{-5}	-	2.2×10^{-4}	-
74	(3.2×10^{-4})[a]	0.0034	1.1×10^{-4}	0.001	4.1×10^{-4}	0.0011
75	(8.8×10^{-4})	0.0062	8.3×10^{-4}	0.0040	7.5×10^{-4}	0.0023
76	(0.0029)	0.012	0.0012	0.0078	0.0014	0.0051
77	0.0083	0.023	0.0038*	0.014	0.0026	0.011
78	0.021	0.048	0.0095	0.026	0.0049	0.025
79	(0.041)	0.096	0.019	0.053	0.0090	0.043
80	(0.077)	0.19	0.045	0.096	0.016	0.075
81	0.14	0.21	0.088	0.18	0.030	0.14
82	(0.29)	0.50	0.20	0.35	0.056	0.23
83	0.544	0.80	0.40*	0.66	0.10	0.37
84	1.00	1.3	0.85*	1.02	0.17	0.60
85	1.30	1.85	0.80	1.45	0.28	0.92
86	2.02	2.5	1.38*	1.9	0.45	1.15
87	(2.94)	3.3	1.90	2.25	0.73	1.5
88	(3.92)	4.2	2.45	2.7	1.2	1.9
89	4.79	5.1	2.9*	3.17	1.9*	2.4
90	5.77	5.8	3.2*	3.7	2.4	3.0
91	5.84	5.85	3.6	4.3	3.0	3.7
92	6.03	6.0	4.1	4.8	3.7	4.4
93	6.45	6.4	4.85	5.2	4.6	5.0
94	6.40	6.4	5.3	5.45	5.5	5.4
95	6.27	6.3	5.7*	5.6	5.9*	5.6
96	6.33	6.3	5.8	5.7	5.7	5.3
97	6.09	6.1	5.7	5.64	5.6*	5.2*
98	5.78	5.8	5.7	5.6	5.4	5.4
99	6.06	6.1**	6.3*	6.2**	5.9*	5.9*
100	6.30	6.7	6.1	6.4	6.0	6.4
101	5.0	5.3	5.5	6.5	6.0	5.9

Table 2.3 (continued)

CUMULATIVE-MASS-CHAIN YIELDS OF FISSION PRODUCTS
(VALUES ARE IN PERCENT OF FISSIONS)

Mass Number	U-235		U-238		Pu-239	
	Thermal Neutrons*	Fission Neutrons	Fission Neutrons	8-Mev Neutrons	Thermal Neutrons	Fission Neutrons
102	4.1	2.9	5.6	5.9	5.9	5.3
103	3.0	1.7	6.6	5.0	5.8*	4.6
104	1.8	0.95	5.4	3.2	5.0	3.5
105	0.90	0.54	3.9	2.2	3.9*	3.2
106	0.38	0.30	2.7*	1.5	5.0*	3.6
107	0.19	0.17	1.35	1.0	4.0	3.1
108	(0.085)	0.095	0.67	0.70	3.0	2.6
109	(0.039)	0.053***	0.32*	0.48	1.5*	1.9*
110	(0.026)	0.030	0.15	0.33	0.65	0.81
111	(0.015)	0.022***	0.073	0.25***	0.27*	0.34
112	(0.013)	0.020***	0.046*	0.19	0.10*	0.14*
113	(0.012)	0.018	0.043	0.17	0.055	0.090
114	(0.011)	0.017	0.041	0.16	0.046	0.075
115	0.0104	0.017***	0.040*	0.15***	0.041*	0.069*
116	(0.010)[b]	0.017[b]	0.039	0.14	0.039	0.065
117	(0.010)	0.017	0.039	0.14[b]	0.038	0.065
118	(0.010)	0.017	0.040[b]	0.14	0.038[b]	0.064[b]
119	(0.011)	0.017	0.041	0.14	0.039	0.064
120	(0.011)	0.018	0.042	0.15	0.041	0.065
121	(0.012)	0.020	0.044	0.16	0.044*	0.066
122	(0.013)	0.022	0.046	0.17	0.047	0.069
123	(0.015)	0.030	0.050	0.19	0.052	0.076
124	(0.017)	0.053	0.055	0.23	0.058	0.082
125	0.021	0.095	0.072	0.33	0.072*	0.14
126	(0.058)	0.17	0.175	0.48	0.175	0.35
127	(0.145)	0.30	0.39	0.70	0.39*	0.80
128	0.37	0.54	0.77	1.0	0.77	1.9
129	0.90	0.95	1.45	1.5	1.45	2.5
130	2.0	1.7	2.5	2.2	2.5	3.2
131	(2.88)	2.9	3.2*	3.2	3.8*	3.8

Table 2.3 (continued)

CUMULATIVE MASS-CHAIN YIELDS OF FISSION PRODUCTS
(VALUES ARE IN PERCENT OF FISSIONS)

Mass Number	U-235		U-238		Pu-239	
	Thermal Neutrons*	Fission Neutrons	Fission Neutrons	8-Mev Neutrons	Thermal Neutrons	Fission Neutrons
132	(4.31)	4.3	4.7*	4.4	5.0	4.6
133	(6.48)	6.1	5.5*	5.4	5.27*	4.9
134	(7.80)	7.3	6.6*	6.5	5.69*	5.2
135	(6.40)	6.3	6.0*	5.9	5.53*	5.1
136	(6.36)	6.4	5.9*	5.8	5.06*	5.3
137	(6.05)	6.0	6.2	5.85	5.24*	6.4*
138	5.74	5.7	6.4	5.9	5.5	5.4
139	(6.34)	6.4	6.5	6.0	5.7*	5.2
140	6.44	6.4	5.7*	5.6	5.68*	5.0*
141	(6.30)	6.3	5.7	5.5	5.2*	4.7
142	(5.85)	5.9	5.7	5.4	5.69*	4.9
143	(5.87)	5.8	5.5	4.97	5.4*	5.0
144	5.67	5.1**	4.9*	4.3**	5.29*	4.8
145	3.95	4.2	3.7	3.7	4.24*	4.4
146	3.07	3.3	3.1	3.17	3.53*	3.7
147	2.38	2.5**	2.6**	2.7**	2.92*	3.0
148	1.70	1.85	2.0	2.27	2.28*	2.36
149	1.13	1.3**	1.45	1.9**	1.75	1.86
150	0.67	0.80	1.05	1.45	1.38*	1.48
151	0.45	0.50	0.74	1.02	1.08	1.16
152	0.285	0.31	0.50	0.66	0.83*	0.92
153	0.15	0.19**	0.32	0.41**	0.52	0.60
154	0.077	0.096	0.19	0.25	0.32*	0.37
155	0.033	0.048	0.11	0.15	0.20	0.23

Table 2.3 (concluded)

CUMULATIVE MASS-CHAIN YIELDS OF FISSION PRODUCTS
(VALUES ARE IN PERCENT OF FISSIONS)

Mass Number	U-235		U-238		Pu-239	
	Thermal Neutrons*	Fission Neutrons	Fission Neutrons	8-Mev Neutrons	Thermal Neutrons	Fission Neutrons
156	0.014	0.023**	0.066*	0.092**	0.12*	0.14
157	0.0078	0.012	0.034	0.057	0.064	0.075
158	0.002	0.0062	0.016	0.032	0.034	0.043
159	0.00107	0.0034**	0.0090**	0.017**	0.020****	0.025
160	3.5×10^{-4}	0.0012	0.0036	0.0085	0.0092	0.011
161	7.6×10^{-5}	4.6×10^{-4}**	9.4×10^{-4}	0.0044**	0.0038****	0.0051

*Seymour Katcoff, Fission-Product Yields From U, Th and Pu, Nucleonics, Vol. 16, No. 4, p. 78-85 (1958).

**L.R. Bunney, E. M. Scadden, J. O. Abriam, and N. E. Ballou, Radiochemical Studies of the Fast Neutron Fission of U-235 and U-238, Second UN International Conference on the Peaceful Uses of Atomic Energy, A/Conf. 15/P/643, USA, June 1958.

***G. P. Ford, J. S. Gilmore, et al., Fission Yields, LADC-3083, 1958.

****L. R. Bunney, E. M. Scadden, J. O. Abriam, and N. E. Ballou, Fission Yields in Neutron Fission of Pu-239, USNRDL-TR-268, 1958, Uncl.

a. Parentheses indicate estimated values or where Katcoff's value was altered in order to adjust the yields to a gross sum of 100 in each peak.

b. Line indicates division of two peaks that was used for individual peak sums.

Figure 2.2
THIN SECTION AND RADIOGRAPH OF A FALLOUT PARTICLE FROM A SMALL-YIELD SURFACE SHOT AT THE NEVADA TEST SITE. THE PARTICLE IS A TRANSPARENT YELLOW-BROWN GLASS WITH MANY INCLUSIONS OF GAS BUBBLES AND UNMELTED MINERAL GRAINS. THE RADIOACTIVITY IS DISTRIBUTED IRREGULARLY THROUGHOUT THE GLASS PHASE OF THE PARTICLE

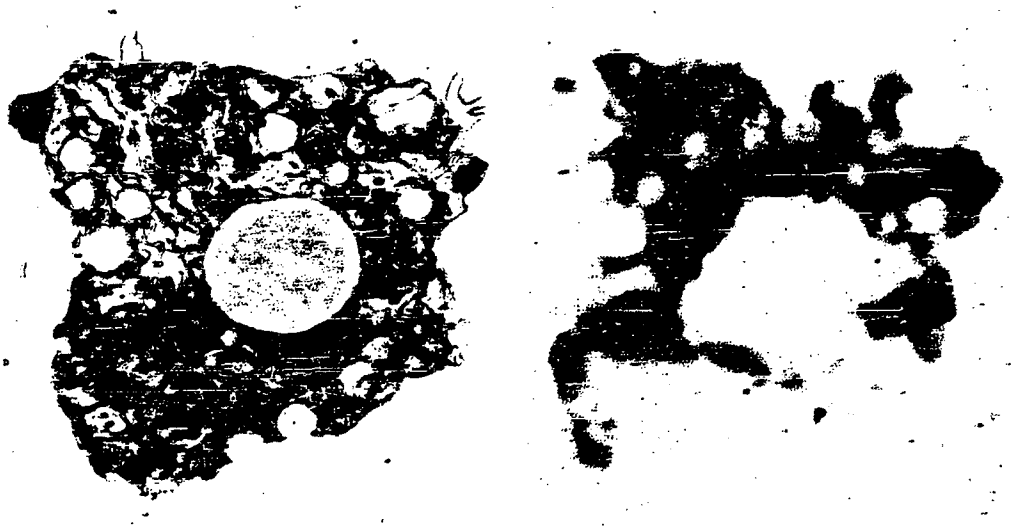

Figure 2.3
THIN SECTION AND RADIOGRAPH OF AN ANGULAR FALLOUT PARTICLE FROM A LARGE-YIELD SURFACE SHOT AT THE ENIWETOK PROVING GROUNDS. THIS PARTICLE IS COMPOSED ALMOST ENTIRELY OF CALCIUM HYDROXIDE WITH A THIN OUTER LAYER OF CALCIUM CARBONATE. THE RADIOACTIVITY HAS COLLECTED ON THE SURFACE AND HAS DIFFUSED A SHORT DISTANCE INTO THE PARTICLE

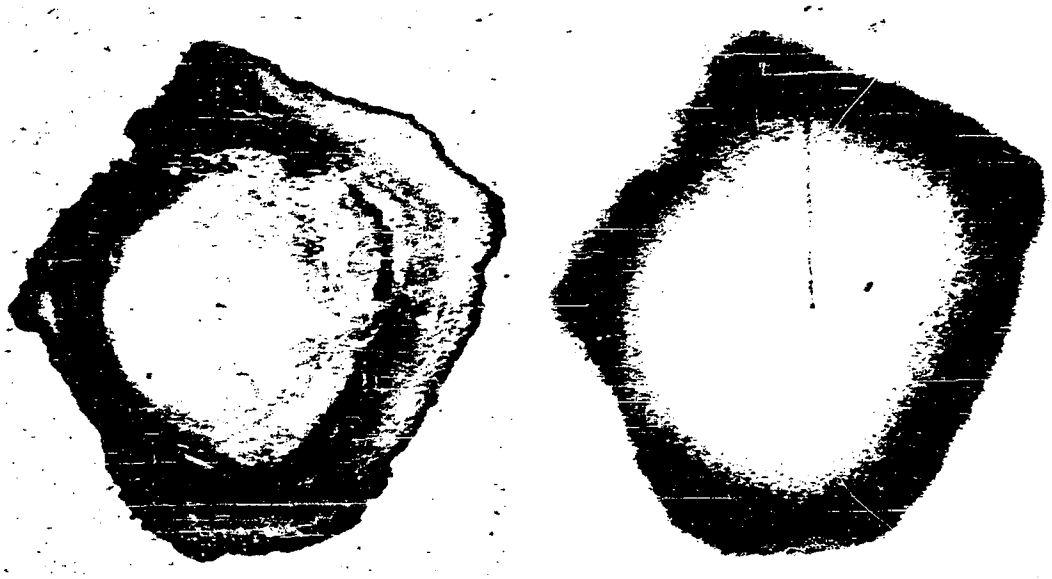

Figure 2.6
TWO FALLOUT PARTICLES FROM A TOWER SHOT AT THE NEVADA TEST SITE. THE PARTICLE ON THE LEFT IS A PERFECT SPHERE WITH A HIGHLY GLOSSY SURFACE; THE ONE ON THE RIGHT HAS MANY PARTIALLY-ASSIMILATED SMALLER SPHERES ATTACHED TO ITS SURFACE. BOTH PARTICLES ARE BLACK AND MAGNETIC AND HAVE A SUPERFICIAL METALLIC APPEARANCE. THE INTERIOR STRUCTURE OF THIS TYPE OF PARTICLE IS SHOWN IN FIGURE 2.7

Figure 2.7
THIN SECTION AND RADIOGRAPH OF A FALLOUT PARTICLE FROM A MODERATE-YIELD TOWER SHOT AT THE NEVADA TEST SITE. THIS PARTICLE IS COMPOSED OF A TRANSPARENT GLASS CORE WITH A DARKLY COLORED IRON OXIDE GLASS OUTER ZONE. MOST OF THE RADIOACTIVITY IS CONCENTRATED IN THE OUTER ZONE

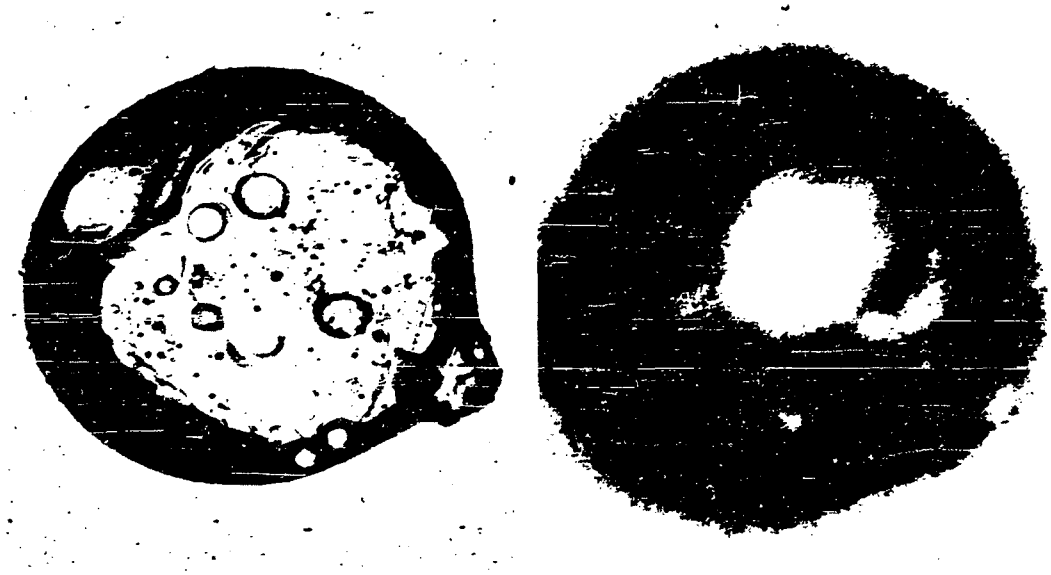

Figure 2.10
PHOTOMICROGRAPH OF A DICHROMATE REAGENT FILM OF AN INDIVIDUAL LIQUID FALLOUT PARTICLE FROM A LARGE-YIELD BARGE SHOT AT THE ENIWETOK PROVING GROUND. THE SOLUBLE CHLORIDE IN THE DROP HAS REACTED WITH THE REAGENT FILM, FORMING A WHITE CIRCULAR AREA INDICATING THE AMOUNT OF CHLORIDE IN THE DROP. THE AREA OF THE CENTRAL ELLIPTICAL TRACE COVERED BY SMALL SOLID PARTICLES IS A MEASURE OF THE WATER CONTENT OF THE DROP. THE SOLIDS IN THE CENTER ARE SMALL SPHERES FORMED BY THE CONDENSATION OF THE VAPORIZED BARGE AND BALLAST MATERIALS

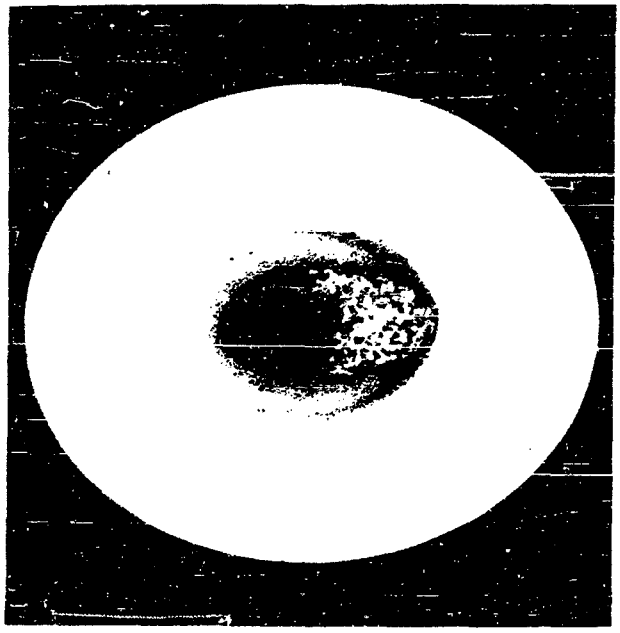

The particle thin-section analyses, although giving much information on the structures of fallout particles and on the way they are formed, give no quantitative data on the radio-chemical composition of the particles, and only a limited amount of unclassified information is available from radio-chemical analyses of fallout particles. The first information of this kind was reported by Kimura[23] et al, who presented analyses of the fallout from Shot Bravo, detonated on March 1, 1954. The fallout for these analyses contaminated the Japanese boat No. 5 Fukuryu Maru. Some of the particles, called ashes or dust because of the white color of calcium carbonate or hydroxide, were collected by the crew of the ship who carried the material back to the Japanese mainland where the analyses were made.

In the report, Kimura chose to refer his data to the thermal-neutron fission of Pu-239. The data were reanalyzed on the basis of 8-Mev neutron fission of U-238 because of the reported high abundance of the nuclide, U-237, presumably produced by a (n, 2n) reaction on U-238. In this instance, the Pu-239 was presumably produced by a (n,γ) reaction on U-238 in which the initial product, U-239, had, to a great degree, decayed to Np-239 and then to Pu-239 by the time of the analyses. Kimura's data are compared with the calculated activities for U-238 fission at D + 25 (25 days after detonation) and summarized in Table 2.4. The ratios of the observed percentages to those calculated for the rare earth nuclides, Y-91 and Nb-95, are greater than one. It is clear that the percentage of fission product activity missing is greater than the 17.45 percent unaccounted for in the sample analyses. To check the reality of the high yield for Nd-147 and the low yield for Ce-141, the two ion-exchange elution curves given by Kimura for the rare earth nuclides at D + 40 were integrated, giving the following percentages: Y-91, 18-21 percent; Pm-147, Nd-147, 3-12 percent; Pr-143, 15-30 percent; and Ce-141, Ce-144, Pr-144, 40-50 percent. These values agree with the calculated percentages of Y-91, 21 percent; Nd-147, 10 percent; Pr-143, 25 percent; and Ce-141, Ce-144, Pr-144, 45 percent, at D + 40. Thus it was concluded that the ratios 0.83 and 2.06 in Table 2.4, for Ce-141 and Nd-147 respectively, do not indicate a depletion of Ce-141 and an enrichment of Nd-147

Assuming that the rare earth elements, yttrium, zirconium, and niobium are in the correct ratios for U-238 fission, their gross contribution to the activity may be used as a basis for estimating the relative depletion or enrichment of other fission-product nuclides. The data of Bolles and Ballou[2] for U-235 fission products (with adjustment to the fission yields of Table 2.3) were used to calculate the percentage of activity at D + 25 for U-238 fission with 8-Mev neutrons. The indicated unfractionated nuclides contribute 46.9 percent of the beta activity, whereas the observed percentage was 65.0 percent; hence only 72 percent of the normal fission-product mixture activity must have been present in the sample. The remaining 28 percent was then either with another group of particles or did not condense on any large fallout particles.

Table 2.4

CALCULATION OF RELATIVE ACTIVITY RATIOS FROM KIMURA'S DATA ON CORAL FALLOUT[23]

Nuclide	Half-Life	Percent Of Total Activity On D+25	Percent Of Fission Product Activity On D+25	Percent Of Activity For U-238 Fission On D+25	Ratio $\left(\frac{\% \text{ Observed}}{\% \text{ For U-238}}\right)$	Adjusted Percent Of Fission Products In Fallout	Fractionation Number r_o (A)
Sr-89	53d	1±0.5	1.25	4.01	0.31	0.90	0.22
Sr-90	28y	0.02±0.01	0.025	0.053	0.47	0.018	0.34
Y-90	61h	0.02±0.01	0.025	0.053	0.47	0.018	0.34
Y-91	57d	8±3	10.0	5.89	1.70*	7.22	(1.0)
Z-95	65d	5±2	6.25	6.94	0.90*	4.51	(1.0)
Nb-95	35d	3±1	3.75	3.06	1.23*	2.71	(1.0)
Ba-140	12.8d	5±1	6.25	11.92	0.52	4.51	0.38
La-140	40h	6±1	7.50	13.39	0.55	5.41	0.40
Ce-141	31d	7±5	8.75	10.55	0.83*	6.31	(1.0)
Ce-144	282d	2±1	2.50	1.49	1.68*	1.80	(1.0)
Pr-143	13.7d	16±5	20.0	12 02	1.66*	14.4	(1.0)
Pr-144	17.5m	2±1	2.5	1.49	1.68*	1.80	(1.0)
Nd-147	11.3d	9±4	11.25	5.46	2.06*	8.12	(1.0)
U-237	6.75d	20±10	-	-	-	-	-
Pu-239	24,360y	$(4\pm2)\times10^{-4}$	-	-	-	-	-
		Sum	82.55				
		Missing	17.45				

* Nuclides with these ratios are assumed to be in correct relative abundance; the ratio of their sums (65.0% of FP activity observed. 46.9% of FP activity for Normal U-238 mixture) is 0.72. The values of r_o(A) are calculated from the ratios of the values of Column 6 to those of Column 4, except for the elements which are assumed to have r_o(A) values of unity.

The ion exchange elution curves reported by Kimura for a gross sample on D + 20 to 22 were also integrated and adjusted to the percentages of the total activity lying under the curve at D + 21. The results are given in Table 2.5, along with the data from Table 2.4 for comparison. In this case, the observed percentage for the rare earth (yttrium, zirconium, and niobium) nuclides is 65.4 percent and the calculated fraction is 43.4 percent; this indicates that, at D + 21, 66 percent of the total activity of the normal mixture was present in the sample. The percentages at the two times differ a little; they would, of course, be expected to change with time.

The estimated fractionation numbers, $r_0(A)$, given in Table 2.6 for various nuclides in the fallout were compiled from the data of Tables 2.4 and 2.5 and other sources as noted. In addition to the rare gas elements and their daughter products, the important elements in the fallout that were depleted include Ru, Te, and I. Other elements undoubtedly were also fractionated but are not listed because they would not contribute significant amounts of activity at D + 21 and D + 25. The summed beta activity for the unfractionated mixture of activities at D + 25 is 7.61×10^{-8} disintegrations per second (d/s) per fission. Since only 72 percent at this amount is present in the fallout sample, the equivalent beta activity at D + 25 is 5.49×10^{-8} d/s per fission.

Pu-239, with a 24,360-year half-life and formed from the decay of U-239 and Np-239, has a decay rate ($1/\lambda$) value of 1.11×10^{12} atoms of Pu-239 per d/s. At D + 25, the reported ratio of the Pu-239 activity to the fission product activity is 5.0×10^{-6}. The product of these values gives 0.3 atoms Pu-239 per fission. This is essentially equal to the number of U-239 atoms formed at zero time.

The ratio of the activity of the U-237 to the fission products at D + 25 is given as 20/80. For the 6.75-day half-life, $1/\lambda$ is 8.42×10^5 atoms U-237 per d/s; hence the relative capture number, C, is

$$C(237) = (20/80) \times 8.42 \times 10^5 \times 5.49 \times 10^{-8} / \exp\left[\frac{-0.693 \times 25}{6.75}\right] \qquad (2.1)$$

$$= 0.15 \text{ atoms/fission}$$

Since the alpha-counting technique and separation methods might result in low values of Pu-239 activity relative to the total, the yield of U-239 (or Pu-239) in the sample could well have been larger than 0.3 atoms per fission. For a broad energy band of neutrons centering at about 8- Mev, the yield from a (n,γ) reaction on U-238 could be as much as 5 times the yield of the (n, 2n) reaction.

Table 2.5

PERCENTAGE ACTIVITIES IN ION EXCHANGE PEAKS OF DIFFERENT CHEMICAL GROUPS IN CORAL FALLOUT SAMPLE[23]

Peak No.	Elements	Percent Of Total Activity At D+21	Percent Of FP Activity At D+21	Percent Of U-238 FP Activity At D+21	Adjusted Percent Of FP Activity At D+21	Adjusted Percent Of FP Activity At D+25
1	Sb, Te, I, Ru, Rh, Mo	13.5	17.2	19.8	11.4	12.6
2	Zr, Nb	8.3	10.6	8.25	7.0	7.2
3	U	21.3	-	-	-	-
4	Y, Ce, La, Pr, Nd, Pm	49.4	62.7(54.8)*	35.2	36.4	39.7
5	Sr (Y)	1.3	1.6	3.61**	1.06	0.92
6	Ba (La)	6.2	7.9(15.8)*	26.1	10.5	9.9

*7.9% for La-140 is added to Peak 6 and subtracted from Peak 4 for calculating the fraction of normal fission-product activity present.

**Includes Sm and Eu as contributing to Sr fraction.

Table 2.6

SUMMARY OF ESTIMATED FRACTIONATION NUMBERS FOR BETA-EMITTING NUCLIDES IN CORAL FALLOUT FROM NO. 5 FUKURYU MARU AT D+21 AND D+25

Fractionation Number, $r_o(A)$				
Nuclide	Note	D+21 data	D+25 data	Selected Value
Kr-85	1	(0)	(0)	0
Sr-89		0.27	0.22	0.22
Sr-90		0.27	0.34	0.34
Y-90		0.27	0.34	0.34
Y-91		1.0	1.0	1.0
Zr-95		1.0	1.0	1.0
Nb-95		1.0	1.0	1.0
Mo-99	1	(1.0)	(1.0)	1.0
Ru-103	1	(1.0)	(1.0)	1.0
Ru-106	2	0.14	0.41	0.41
Rh-106	2	0.14	0.41	0.41
Ag-111	1	(1.0)	(1.0)	1.0
Cd_i-115	1	(1.0)	(1.0)	1.0
Cd_g-115	1	(1.0)	(1.0)	1.0
In-118	1	(1.0)	(1.0)	1.0
Sn-123	1	(1.0)	(1.0)	1.0
Sn-125	1	(1.0)	(1.0)	1.0
Sb-125	1	(1.0)	(1.0)	1.0
Sb-127	1	(1.0)	(1.0)	1.0
Te-127	1	(1.0)	(1.0)	1.0
Te-129	2	0.09	0.27	0.27
Te-132	2	0.06	0.19	0.19
I-131	2	0.08	0.24	0.24
I-132	2	0.06	0.19	0.19
Xe-133	1	(0)	(0)	0
Cs-137	3	--	0.23	0.23
Ba-140		0.40	0.39	0.40
La-140		0.40	0.53	0.46
Ce-141		1.0	1.0	1.0
Ce-144		1.0	1.0	1.0
Pr-143		1.0	1.0	1.0

Table 2.6 (concluded)

SUMMARY OF ESTIMATED FRACTIONATION NUMBERS FOR BETA-EMITTING NUCLIDES IN CORAL FALLOUT FROM NO. 5 FUKURYU MARU AT D+21 AND D+25

Fractionation Number, $r_0(A)$				
Nuclide	Note	D+21 data	D+25 data	Selected Value
Nd-147		1.0	1.0	1.0
Pm-147		1.0	1.0	1.0
Sm-151		1.0	1.0	1.0
Sm-153		1.0	1.0	1.0
Eu-155		1.0	1.0	1.0
Eu-156		1.0	1.0	1.0

Note 1: Estimated

Note 2: Estimated from ion exchange elution peak activity percentage and from data of Section 2.8, giving the relative fractions condensed of mass numbers 132, 131, 129, and 106, considered to be in the ratio of 1 : 1.3 : 1.4 : 2.2.

Note 3: From a plot of $r_0(A)$ versus the half-life of rare-gas precursors.

It may be noted that, at D + 25, the relative activity of 56-hour Np-239 is 2.06×10^{-9} d/s per atom of U-239 produced initially, and for 6.75-day U-237 it is 9.13×10^{-8} d/s per atom of U-237. Thus, even at a 5-to-1 yield ratio, the activity of the Np-239 at D + 25 would be only 1/8 of the U-237 activity and would be difficult to detect. The factor of 5 would give a capture number, C(239), value of 0.75 atoms per fission.

The second set of unclassified data on the radiochemical content of radioactive particles was reported by Mackin and coworkers at NRDL.[24] The sample particles were obtained from detonations on coral islands at the Eniwetok Proving Grounds in 1956. In this case, analyses are made for only a few radionuclides: Mo-99, Sr-89, Ba-140, and Np-239. However, no Np-239 data are reported. In addition, the gross activity of the particles is measured by using a well-crystal (WC) NaI(Tl) scintillation counter and a 4π high-pressure argon gas (at a pressure of 600 psig) gamma ionization chamber.[25]

Many of the particles were weighed so that specific activities could be determined, and some data on gross samples were obtained. The Mo-99 radionuclide was utilized as the "fission" tracer with the assumed yield of 6.1 percent; this yield value is sufficiently close to the yield for the 8-Mev neutron fission of U-238 that no adjustment of the reported values was required. Some of the data are summarized in Table 2.7. The particle type designations "altered" and "unaltered" used by the authors have been changed to "fused" particles and "irregular" particles as the first classification of the particles as the first classification of the particle type since the thin-section analyses showed that most of the irregular particles have been calcined.

Because of analytical requirements, only the more highly radioactive particles were used in the reported analyses. This means that the results are applicable only to a description of the larger particles. However, even with this bias, the results are useful in illustrating the possible range in values of all the measured quantities.

The counting-rate and ion-current measurements were corrected to 11470 hours before the apparent average ionization rates, WC-rates per fission, ion current per fission, and the specific ionization rate were computed. The decay corrections for the WC measurements were obtained from the reported decay curves for the two types of particles; the ionization rate decay corrections were obtained from unpublished data on particles from the same set of samples. It is quite likely that each particle had its own decay rate, differing to some degree from other particles of the same general type. Therefore, with a single type of decay curve, the corrections to a common time are only approximate.

The variability of the ratio of the ion current to the WC count-rate of the set of particles is the first indication of a gross difference in the relative abundances of the emitted gamma rays of different energies, hence of a

Table 2.9

SUMMARY OF FRACTIONATION NUMBERS RELATIVE TO MASS NUMBER 99 FOR CORAL AND SEAWATER FALLOUT CORRECTED FOR APPROPRIATE FISSION YIELDS

	Relative Sample Location	Mass Number									
		89	90	95	99	132	137	140	144	237[a]	239[a]
	A. Larger Yield (MT Range) Coral Surface Detonation										
Increasing Distance from Shot Point	Cloud Sample ↓	5.1	4.0	2.1	(1.0)	2.5	3.3	4.2	2.0	1.2	1.2
		0.83	0.97	1.6	(1.0)	1.3	-	-	1.5	0.91	0.98
		0.38	0.44	1.0	(1.0)	0.69	0.22	0.88	0.96	0.78	0.87
		0.031	0.079	0.94	(1.0)	0.12	0.020	0.14	0.95	0.71	0.75
		0.13	0.24	0.82	(1.0)	0.45	0.046	-	0.88	0.73	0.75
		0.056	0.093	1.0	(1.0)	0.15	0.013	-	0.65	0.74	0.81
	B. Large Yield (MT Range) Shallow Water Surface Detonation (Coral Bottom)										
Increasing Distance from Shot Point	Cloud Sample ↓	2.1	2.1	1.4	(1.0)	1.5	1.7	2.2	1.2	1.0	1.0
		0.42	0.57	1.1	(1.0)	0.94	0.37	-	1.2	0.87	0.92
		0.65	0.74	1.5	(1.0)	1.3	0.20	-	1.6	1.0	1.1
		0.38	0.49	0.92	(1.0)	0.81	0.13	0.86	0.89	0.77	0.82
		0.082	-	0.51	(1.0)	0.27	-	-	0.60	0.56	0.63
		0.24	0.36	0.84	(1.0)	0.48	0.13	-	0.81	0.70	0.76
		0.12	0.18	0.84	(1.0)	0.34	0.062	0.42	0.70	0.72	0.71

a. Values for 237 and 239 are not corrected for yields.

Table 2.9 (concluded)

	Relative Sample Location	Mass Number									
		89	90	95	99	132	137	140	144	237[a]	239[a]
	C. Medium Yield (KT Range) Surface Detonation on Deep Water										
Increasing Distance from Shot Point	Cloud Sample	2.6	1.7	0.90	(1.0)	1.0	2.5	1.6	0.96	1.0	0.98
	↑	0.73	-	1.0	(1.0)	1.1	0.42	-	1.1	1.0	0.97
		0.79	0.78	0.94	(1.0)	0.87	0.38	-	0.90	0.99	0.84
		0.46	0.47	1.3	(1.0)	0.98	-	0.70	1.1	1.1	0.98
		0.51	0.51	1.0	(1.0)	1.0	0.20	0.90	0.94	1.0	1.1
		0.30	0.57	1.1	(1.0)	0.99	-	-	1.0	1.1	0.98
	D. Large Yield (MT Range) Surface Detonation on Deep Water										
Increasing Distance from Shot Point	Cloud Sample	1.1	-	1.2	(1.0)	0.77	-	1.0	1.0	0.98	1.0
	↑	1.2	0.99	1.1	(1.0)	1.0	-	-	1.3	0.94	0.97
		0.96	0.93	1.1	(1.0)	0.95	0.41	-	0.92	0.86	0.96
		0.90	0.94	0.92	(1.0)	1.0	1.0	-	1.0	1.1	1.1
		0.53	0.80	1.5	(1.0)	1.0	1.2	-	1.1	0.64	0.71
		0.90	1.2	1.3	(1.0)	1.1	-	-	1.4	0.72	0.74
		1.6	1.2	0.95	(1.0)	1.1	-	-	0.94	0.72	0.74

Table 2.12

AVERAGE FRACTIONATION NUMBERS OF RADIONUCLIDES IN FALLOUT FROM TOWER AND BALLOON-SUPPORTED DETONATIONS AT THE NEVADA TEST SITE

Nuclide	R(95)[a]	
	Tower	Balloon
Sr-89	0.32	1.5
Sr-90	0.65	-
Y-91	1.4	2.8
Zr-95	1.0	1.0
Ru-103(106)	0.45	3.2
Ba-140	1.4	3.5
Ce-141(144)	1.4	2.3

a. Relative to the yields for thermal neutron fission of U-235.

Table 2.13

GROSS SOLUBILITY OF ACTIVITY FROM SMALL FALLOUT PARTICLES

Type of Detonation	Percent Activity Soluble[a]		Particle Size (microns)
	in H_2O	in 0.1N HCl	
Underground	5.4	25	0-44
Tower-Mounted	2	14 to 36	0-44
	1	5	44-ca 100
Balloon-Supported	14	60	0-44
	31	90	44-ca 100

a. Based on beta count-rate measurements (presumably at about 2 weeks after detonation).

than were condensed in this manner in the tower detonation. The higher solubility of the activity in acid, especially for the air burst fallout, may be partially due to dissolution of the primary iron oxide or alumina particles. However, the very high solubility in both water and acid of the radioactivity on the larger particles from the air burst suggests almost complete surface

Table 2.14

GROSS SOLUBILITY OF ACTIVITY FROM SMALL FALLOUT PARTICLES LODGED ON PLANT FOLIAGE

Plant Type	Distance From Ground Zero (miles)	Fraction Dissolved[a] in 0.1N HCL
1. Shot Apple I (14 KT on 500 ft. Tower)		
Artemisia (Sagebrush)	12	0.20
Ephedra (Mormon tea bush)	40	0.27
Ephedra (Mormon tea bush)	80	0.15
Juniperus (Juniper)	165	0.32
	Average:	0.24
2. Shot Met (22 KT on 400 ft. Tower)		
Larrea (Creosote bush)	20	0.26
Larrea (Creosote bush)	58	0.08
Medicago (Alfalfa)	140	0.14
	Average:	0.16
3. Shot Apple II (29 KT on 500 ft. Tower)		
Triticum (wheat)	7	0.19
Triticum (wheat)	40	0.17
Triticum (wheat)	106	0.35
	Average:	0.24

a. Based on beta count-rate measurements.

weathering factor of 0.4 due to the first heavy rains 10 to 20 days after the first detonation, apparently by comparison with an inappropriate decay curve. This misinterpretation has also been noted by Knapp[40] in discussions of this subject.

Experimental measurements reported by Miller and Reitemeier[10] on soluble radionuclides deposited on soils through which water has passed gave an average leaching depth, for Sr-89, of 0.75 inch after passing 30 inches of water, and 1.5 inches after passing 300 inches of water. The movement of Cs-137 is found to be only 0.25 inch after passage of 300 inches of water, even in sandy soil. Larson and Neel[29] report penetrations up to 0.5 inch after the passage of 84 inches of water; the source of the activity used in the experiments was not specified.

These data show that the soluble radionuclides, in almost all cases, would be absorbed by the top inch or two of soil particles and remain there unless the whole layer eroded away in heavy rains. But even in this case the nuclides would remain attached to the particles; the fraction of the nuclide soluble in water in such conditions would be negligibly small. The studies of Thornthwaite, Mather, and Nakamura[41] show that many rain cycles would be needed to transport the activity farther than about two inches below the surface of the soil. Since most of the radioactivity on the larger fallout particles would be fused into the particles, the only way it could move into the soil is by mechanical mixing, as occurs in the plowing or discing of agricultural lands.

The translocation of fallout particles on land areas by wind occurs to a small degree. The experience in the Nevada Test Site, (under dry conditions) where excursions in the fallout area were made by experimental crews to recover fallout samples, was that, for entries during the first day after a detonation, clothes became contaminated with small fallout particles due to the stirring up of surface dusts and brushing against desert plants, but that, for entries after the second day or so, only the bottom parts of shoes (or booties) picked up fallout particles. Apparently the small particles become adsorbed or physically attached to larger particles, or otherwise become mechanically trapped by the surface soil grains.

Movement of large particles by the wind is usually small because the larger gravity force retards such movement. However, particles in the size range of about 100 to 300 microns drift more easily than particles of other diameters if the surface wind speed is in excess of about 10 mph. These particles, if dislocated, may carry with them small attached fallout particles. Data from experiments at Camp Parks, California, reported by Sartor and Owens[42] in which particles with diameters from 150 to 300 microns (tagged with Ba(La)-140) were deposited on various types of surfaces showed that the movement of the particles on unpaved areas and on tar and gravel roofs is insignificant, even for wind speeds up to 20 mph. The movement of the particles on and from paved

areas is found to be quite large; the particles apparently moved in the wind by hopping and by rolling over the smooth surfaces, although very few particles were raised higher than 3 or 4 inches. They did not jump over curbs but were deposited along the gutters and in depressions and behind low obstructions.

The fraction of the original ionization rate remaining, as measured in the center of a street and in the center of a rather large area of asphaltic concrete, is plotted in Figure 2.14 as a function of the total wind vector (including only winds in excess of 10 mph) that occurred over a ten-day period. Further data of this kind on other particle sizes are needed to establish whether the data of Figure 2.14 are representative of the reductions that could occur generally in the ionization rate at locations of interest. The reduction in the ionization rate for both areas in the first four days (wind vector of 200 miles) was equivalent to a decontamination of about 50 percent; some of this, of course, was due to shielding, since the particles concentrated in surface depressions and along barriers.

2.6 The Collection and Retention of Fallout Particles by Plant Foliage

Some of the data obtained at weapons' tests on the collection and retention of fallout particles by foliage are reported by Romney, Lindberg, Hawthorne, Bystrom, and Larson.[33] Their stated findings, with respect to the ability of the outer surface of leaves to trap and retain fallout particles, were that the size-range of particles lodged on the foliage was predominately less than 100 microns in diameter and that the best correlations of the amount of activity (beta count-rate) on the foliage was with the fraction of the total activity carried by particles having diameters less than 44 microns that landed at the same location. These two findings suggest that the foliage of most plants is selective in trapping only the smaller sizes of fallout particles. Some of the reported data are given in Table 2.15, as converted from curie units at H+12 to the equivalent number of fissions by use of the factor, 5.67×10^9 fissions/microcurie.[26] The median particle diameters are taken from the plotted particle-size distributions in Figure 2.15.

It is interesting that the median particle diameter increased with fallout arrival time up to arrival times of 4 to 5 hours after detonation. However, since the data are for different plant species, part of this increase also may be due to the plant species selected for analysis. The spread of the distributions, however, tend to decrease with time of fallout arrival or with decreasing particle size of the arriving fallout. The upper-limit particle diameter cut-off is fairly sharp at diameters larger than 88 microns, excepting for the bushmallow foliage sample. The higher retention levels and larger particles on the bushmallow foliage is probable due to the high density of stellate hairs on the leaves which would serve to trap and hold particles onto the surface.

Figure 2.14
REDUCTION IN THE IONIZATION RATE AT THE CENTER OF 10TH STREET AND AT THE CENTER OF THE PLAZA, CAMP PARKS, CALIFORNIA; AS A FUNCTION OF THE WIND VECTOR (sum of the products of wind speed × time) FOR WINDS IN EXCESS OF 10 MPH OVER A 10-DAY PERIOD. THE TAGGED PARTICLES WERE 150 TO 300 MICRONS IN DIAMETER

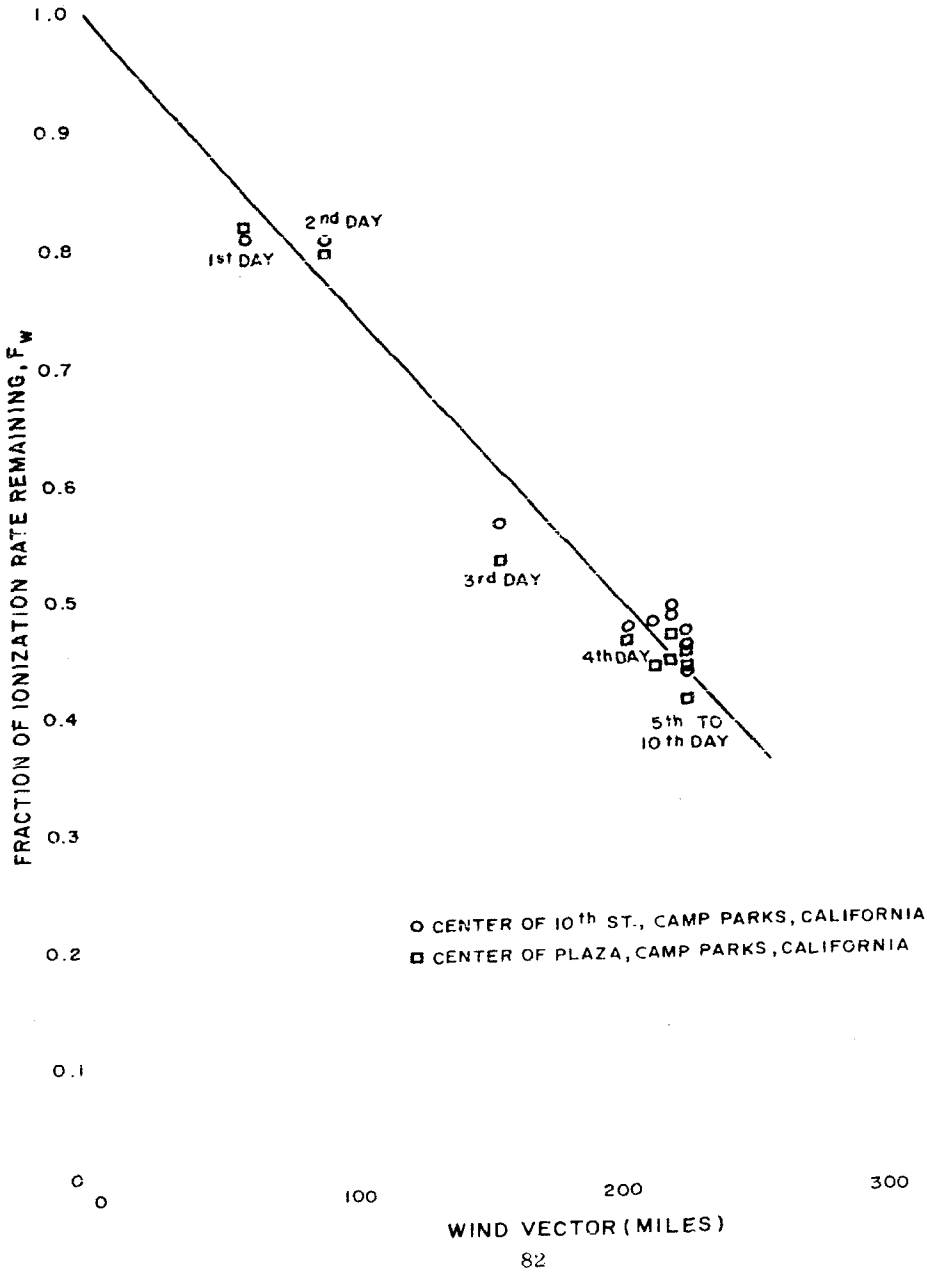

Figure 2.15
ACCUMULATED DISTRIBUTION OF THE NUMBER OF PARTICLES WITH DIFFERENT DIAMETERS ON FOLIAGE

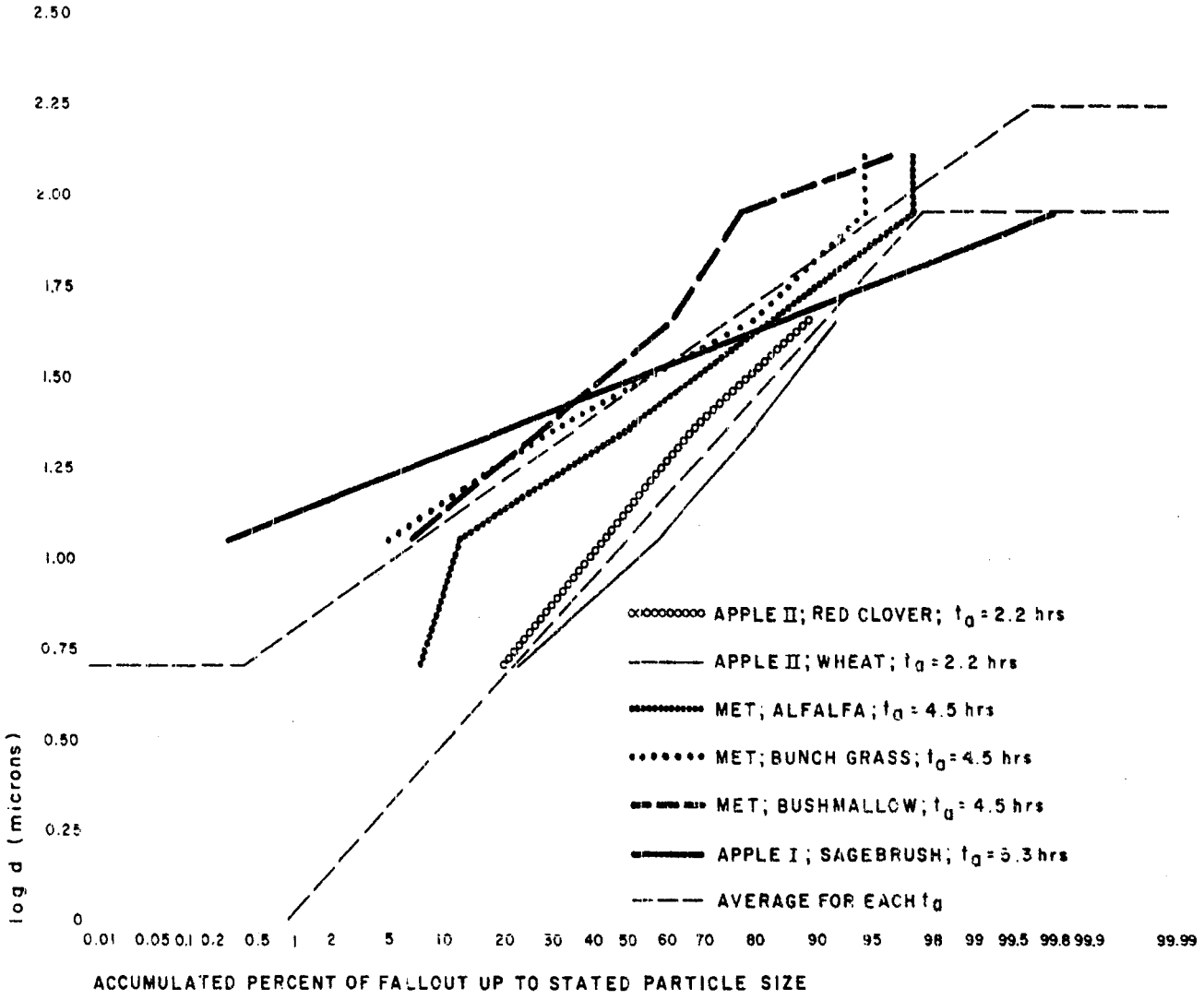

Data on the collection of the fallout from Apple II shot and Smoky shot tower detonations by some forage crops are given in Table 2.16. The fractions of the deposited fallout retained by red clover (in flats) increased with time of fallout arrival from about 0.1 percent at 7 miles downwind from the Apple II shot to about 1 percent at 106 miles away. For wheat, the fractions retained increased from about 0.2 percent to about 6 percent over the same range in distance. The highest fraction retained, of these data, was for alfalfa foliage at 259 miles away from shot Smoky. The distributions of the activity on the fallout particles that were deposited at several of the locations are plotted in Figure 2.16. The values of the median diameters decrease with time of arrival as would be expected but the spread of the various activity-size distributions appears to be roughly the same, in logarithmic units, in all the collected samples.

The major conclusion from the data of Romney and coworkers is that the fraction of the deposited fallout collected and retained by foliage is rather small even when the diameters of the arriving particles are small enough to be trapped by the hairs and resins on the leaves. Thus large trees and shrubs cannot be considered as significant sources of radiation where heavy fallout deposits from land surface detonations occur and where the particle diameters are in excess of about 50 microns.

There are no good data on the decontamination of fallout particles from foliage (neglecting data on the very fine material of world-wide fallout). Romney and coworkers,[43] however, do report data on the decontamination of fallout particles from foliage; these can be used to indicate at least the upper limit of a decontamination by a heavy rain. The results of the experiments, using the decontamination reagents water, 0.1 normal HCl and 5 percent EDTA, are summarized in Table 2.17. The water decontamination data would be most representative of the decontamination that could result in a heavy rain. The desert foliage decontaminated generally to levels between about 30 and 40 percent of the initial deposit. However, the smooth-leaf annual was decontaminated to 2 percent and growing wheat was decontaminated to about 20 percent of the initial level. The latter value should be representative of most grass-type foliage

The foliage contamination data appear to show that all the leaves on a plant retain about the same level of contamination on all the foliage. If exceptions to this rather uniform distribution on plant foliage can occur, they conceivably would be most predominant in foliage growths such as a very dense tall growth of grass. This interpretation of the contamination process at least agrees better with the observations than a process in which only the exposed surfaces of the exterior or upper leaves are assumed to be the only collecting surfaces. The use of the assumption of uniform contamination of all the foliage on a plant allows correlation of the fallout particle retention data in terms of the mass of the collecting foliage on a plant. The correlation of the fallout retained per unit

of dry plant (leaf) mass with the total amount of fallout deposited at a location can then be used to evaluate the internal radiological hazard from the intake of radionuclides in the fallout retained on foliage. To make the correlations, a foliage contamination factor, a_L, is defined as the ratio of the number of fissions per gram of dry plant (foliage) to the number of fissions of total fallout per sq. ft. of soil surface. If the plant or foliage surface density is defined as w_L in grams of dry foliage per sq. ft. of soil surface, the fraction of the fallout retained by foliage is

$$F_L = a_L w_L \frac{(\text{fissions/ft}^2 \text{ on foliage})}{(\text{fissions/ft}^2 \text{ on soil})} \qquad (2.5)$$

The denominator quantity, fissions/ft^2 on soil is the total fallout deposit uncorrected for the amount on the foliage. The value of w_L is a measure of the density of plants growing on the land. The values of a_L and a^*_L (for only particles with diameters less than 44 microns) reported by Romney and co-workers[32] are given in Table 2.18 for native desert-type foliage. The independence of the values of a^*_L on distance from ground zero is further evidence of the selectivity of the foliage in retaining only the smaller particles. The high values of a^*_L for the fallout from Shots Met, Diablo, and Shasta could be due either to higher humidity conditions and early post-shot plant collections or to the fact that the fallout from these detonations contained a fairly large fraction of the activity on particles with diameters between 44 and 88 microns which were retained by the foliage.

For general use, the value of a_L is a more important quantity than a^*_L. The dependence of the values of a_L on several detonation parameters and further analysis of the data presented in this section are given in Chapter 6 in the form of fallout contour ratio scaling functions. In most of the data of Table 2.18, the values of a_L increase with distance from ground zero.

It was previously mentioned that, for 100 percent retention of the fallout on clover, the predominance of the direct uptake path for animals eating contaminated clover might be on the order of 3500 to 5000 times greater than that of eating new clover on contaminated soil. However, for foliage conditions where the value of a_L is 1.0×10^{-3} and w_L is 10, the factor of predominance for the direct-uptake path is reduced to the order of 35 to 50. Thus the direct-uptake path, at least for exposure times of about a year, can be expected to be the predominating source of an internal hazard to animals and humans after a nuclear war in which land-surface explosions take place.

Figure 2.16
DISTRIBUTION OF ACTIVITY AS A FUNCTION OF PARTICLE DIAMETER FOR LOCAL COLLECTIONS OF FALLOUT FROM TOWER-MOUNTED DETONATIONS

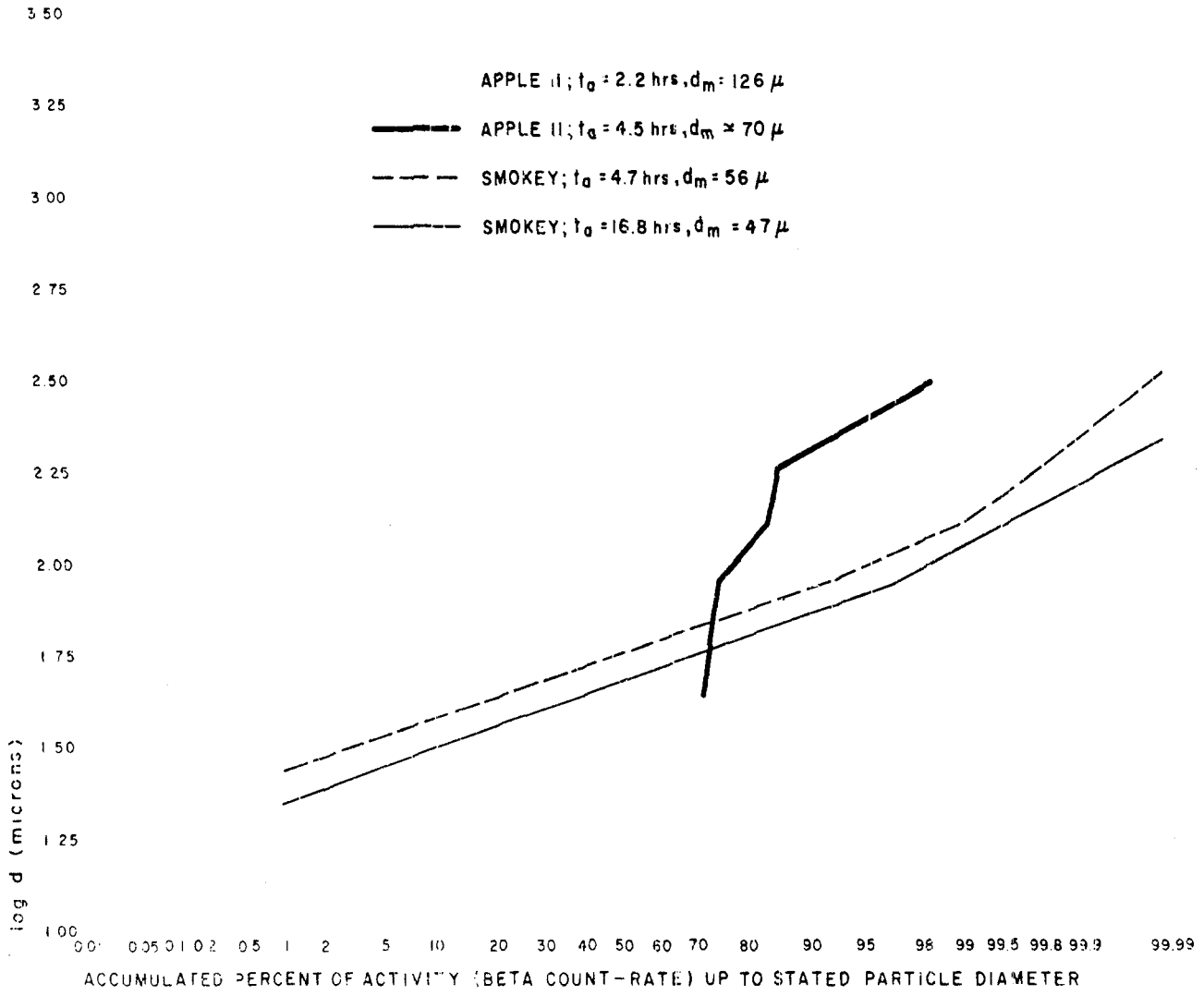

Table 2.15

SIZE DISTRIBUTION AND AMOUNT OF FALLOUT PARTICLES LODGED ON THE FOLIAGE OF DIFFERENT SPECIES OF PLANTS

Quantity	Quantity Value for Designated Plant					
Description of Plant	Artemisia (Sagebrush)	Sphaeralcea (Bushmallow)	Orysopsis (Bunch Grass)	Alfalfa	Red Clover	Wheat
Nuclear Shot	Apple I	Met	Met	Met	Apple II	Apple II
Yield (KT)	14	22	22	22	29	29
Type of Shot	Tower	Tower	Tower	Tower	Tower	Tower
Height of Burst (ft)	500	400	400	400	500	500
Mid-Height of Cloud (ft)	27,050	35,500	35,500	35,000	38,500	38,500
$t_{\frac{1}{2}}$ (Hours)	5.3	4.5	4.5	4.5	2.2	2.2
Particles/cm² of Leaf Surface	10	24	6.8	5.4	3.6	2.3
Fissions/ft² of Leaf Surface	0.79×10^9	30×10^9	1.1×10^9	1.6×10^9	1.2×10^9	0.79×10^9
Fissions/particle (Average)	0.83×10^5	13×10^5	1.8×10^5	3.2×10^5	3.6×10^5	3.7×10^5
Median Particle Diameter	30μ	35μ	29μ	22μ	13μ	9.4μ
Particle Diameter (μ)	Accumulated Distribution of Particle Size on Foliage (Percent)					
0 to 5	0	0	0	7.5(2.5)[a]	19.6	22.5(21)
5 to 11	0	6.9	5.0	12.5(8)	43.5	57.5(50)
0 to 22	38.2	27.6	30.0	50.0(36)	67.4	80.0(74)
0 to 44	84.8	62.0	86.0	82.5(75)	89.1	92.5(91)
0 to 88	100.0	79.2	95.0	97.5(91)	100.0	100.0(100)
0 to 125		96.4	95.0	97.5(96.3)		
0 to 177		100.0	100.0	100.0(100)		
0 to 250						

a. Numbers in parentheses are average values for all types of foliage at the location

Table 2.16

COLLECTION AND RETENTION OF FALLOUT BY SOME FORAGE CROPS

Quantity	Apple II Shot			Smoky Shot		
Yield (KT)		29			44	
Type of Shot		Tower			Tower	
Height of Burst (ft)		500			700	
Mid-Height of Cloud (ft)		38,500			32,000	
t_A (ft - hrs)	0.3	2.2	4.5	4.7	11.8	11.5
X (miles) from ground zero	7	48	106	132	205	259
Y (miles) from bot line	0.6	0.8	34	9.5	0	3.5
Fallout Deposit (fissions/ft^2)	1.17×10^{13}	3.60×10^{12}	1.13×10^{11}	4.25×10^{11}	7.54×10^{11}	4.79×10^{11}
Fallout Lodged on Plant Foliage (fissions on foliage/ft^2 of soil surface)						
Red Clover[a]	1.33×10^{11}	2.39×10^{10}	1.42×10^{9}	-	-	-
Wheat[a]	2.35×10^{11}	8.55×10^{10}	6.58×10^{9}	-	-	-
Alfalfa[b]	-	-	-	2.10×10^{10}	-	5.61×10^{10}
Mixed Grasses[b]	-	-	-	-	2.83×10^{10}	2.55×10^{10}
Fraction of Activity (Beta-Count-Rate) Lodged on Foliage						
Red Clover	1.1×10^{-3}	6.6×10^{-3}	1.25×10^{-2}	-	-	-
Wheat	2.0×10^{-3}	2.37×10^{-2}	5.80×10^{-2}	-	-	-
Alfalfa	-	-	-	4.93×10^{-2}	-	0.117
Mixed Grasses	-	-	-	-	3.75×10^{-2}	5.32×10^{-2}
Surface Density of Foliage (gm. dry plant/ft^2 of soil surface)						
Red Clover	19.6	15.6	15.1	-	-	-
Wheat	33.8	39.6	32.4	-	-	-
Alfalfa	-	-	-	19.2	-	27.9
Mixed Grasses	-	-	-	-	-	16.5
Accumulated Percent of Activity (Beta-Count-Rate) Up to Stated Particle Diameter For the Fallout Deposited at The Location						
Particle Diameter (μ)						
0 to 44	0.15	15.26	71.67	21.11	41.82	No
0 to 88	0.24	17.42	75.74	92.23	96.96	Fallout
0 to 125	0.29	42.40	84.58	99.07	98.86	Sample
0 to 179	0.38	91.72	86.84	99.81	98.96	
0 to 250	0.45	94.51	96.32	99.96	100.00	
250	100.00	100.00	100.00	100.00		

a. Plants were grown in flats of soil and placed at location 1 day before detonation.

b. Plants were collected from farms in the fallout area.

Table 2.17

THE DECONTAMINATION OF FALLOUT PARTICLES FROM FOLIAGE

Plant	Distance From Ground Zero (miles)	Fraction of Gross Activity Remaining on the Foliage After Decontamination[a]		
		Reagent		
		Water	0.1N HCL	5% EDTA
1. Shot Met (22 KT on a 400 ft. Tower)				
Larrea (Creosote bush)	20	0.52	0.34	0.33
Lepidium (Peppergrass)	58	0.19	0.10	0.05
Artemisia (Sagebrush)	140	0.64	0.51	0.46
2. Shot Apple II (29 KT on a 500 ft. Tower)				
Broad-leaf annual	7	0.022	0.18	0.28
Coleogyne (Black brush)	7	0.38	0.18	0.28
Triticum (wheat)	48	0.18	0.10	0.19
Artemisia Spinescens (Sagebrush)	48	0.32	0.16	0.17
Artemisia Tridentata (Sagebrush)	48	0.33	0.20	0.14
Chrysothamnus (Rabbit brush)	48	0.38	0.29	0.10
Atriplex (Shadscale)	106	0.26	0.26	0.21
Chrysothamnus (Rabbit brush)	106	0.40	0.26	0.11

a. Based on beta count-rate measurements

Table 2.17 (concluded)

Leaf Surface Properties
Larrea - very-resinous
Lepidium - glabrous and glaucous
Artemisia - dense, matted, unbranched hairs and glands
Broad-leaf annual - smooth, veined, sparse hairs
Coleogyne - dense, fine hairs
Triticum - rows of short hairs, parallel to veins
Chrysothamnus - dense, soft, wooly hairs
Atriplex - scurfy surface
Ephidra - scale-like, muricated branches
Juniperus - scale-like, imbricated
Oryzopsis - sparse, barb-like hairs
Sphaeralcea - dense, stellate hairs
Trifolium (clover) - rough, with scattered, unbranched hairs

Table 2.18

SUMMARY OF AVERAGED FOLIAGE CONTAMINATION FACTORS FOR NATIVE FOLIAGE EXPOSED TO FALLOUT FROM TOWER- AND BALLOON-MOUNTED DETONATIONS AT THE NEVADA TEST SITE

Shot	Distance from Ground Zero (miles)	$10^3 \, a_L$ (fissions/gm of dry plant / fissions/ft^2 of total fallout)	$10^3 \, a^*_L$ (fissions/gm of dry plant / fissions/ft^2 of $\leq 44\mu$ fallout)
Tesla, 1955	12	0.008	2.23
	60	0.413	2.21
	79	0.453	2.26
	96	0.524	2.09
Apple I, 1955	12	0.355	2.78
	40	0.823	2.36
	80	0.465	2.02
Met, 1955	20	0.625	12.64
	80	2.37	18.00
	140	2.65	18.23
Apple II, 1955	7	0.002	2.39
	48	0.720	2.32
	106	0.97	2.00
Priscilla, 1957[a]	7	4.30	5.06
	84	2.28	7.27
	129	5.12	6.42
	154	5.20	6.46
	190	4.30	6.16
Diablo, 1957	12	1.91	23.8
	15	1.79	39.0
	20	1.63	17.8
	40	6.23	12.2
	62	12.9	16.5
Shasta, 1957	15	1.52	11.6
	44	1.87	7.72
	76	2.81	5.62
	172	8.10	9.42
Smoky, 1957	48	0.460	2.98
	80	0.373	2.52
	100	0.250	2.85

Table 2.18 (concluded)

Shot	Distance from Ground Zero (miles)	$10^3 \, {}^{a}L$ / (fissions/gm of dry plant / fissions/ft^2 of total fallout)	$10^3 \, {}^{a}L$ / (fissions/gm of dry plant / fissions/ft^2 of $<44\mu$ fallout)
	136	0.529	2.76
	158	1.40	3.12
	175	1.29	2.90
	206	0.932	3.28

a. Balloon-mounted detonation

CHAPTER 2 REFERENCES

1. The Effects of Nuclear Weapons, U.S. Government Printing Office, Washington 25, D.C.(1957)

2. Bolies, R. C., and N. E. Ballou, Calculated Abundances of U-235 Fission Products, USNRDL-456, 1956

3. Glendenin, L. E., Technical Report No. 35, Massachusetts Institute of Technology, Cambridge, Mass., 1949

4. Present, R. D., Phys. Rev., 72, 7 (1947)

5. Katcoff, Seymour, Nucleonics, 16, 4, 78 (1958)

6. Steinberg, E. P., L. E. Glendenin, International Conference on The Peaceful Uses of Atomic Energy, 7, 3 (1956)

7. Pappas, A. C., International Conference on The Peaceful Uses of Atomic Energy, Vol. 15, 583 (1958)

8. Wahl, A. C., J. Inorg. Nucl. Chem. 6, 263 (1958)

9. Glendenin, L. E., C. D. Coryell, and R. R. Edwards, Radiochemical Studies: The Fission Products, NNES, Plutonium Project Record, Div. IV, 9, 489, McGraw Hill, New York, N.Y., 1951

10. Herrington, A. C., Massachusetts Institute of Technology, Laboratory for Nuclear Science, Annual Progress Report, p. 37, June 1957-June 1958

11. Miller, C. F., A Theory of Formation of Fallout, USNRDL-TR-425, 1960

12. Adams, C. E., I. G. Popoff, and N. R. Wallace, The Nature of Individual Radioactive Particles, I. Surface and Underground ABD Particles from Operation Jangle, USNRDL-374, 1952

13. Maxwell, Ray D., Project 2.5a-3 Report, Operation Jangle, 1952

14 Schorr, M. G., and E. S. Gilfillan, Project 2.0 Report, Operation Jangle, 1952

15. Alexander, L. T., J. M. Blume, and M. E. Jefferson, Project 2.8 Report, Operation Jangle, 1952

16. Stewart, K., Trans. Faraday Soc. 52, 161 (1956)

17. Pettijohn, F. J., Sedimentary Rocks, Harper Brothers, New York, N.Y., 1949

18. Adams, C. E., The Nature of Individual Radioactive Particles, II. Fallout Particles from M-Shot, Operation Ivy, USNRDL-408, 1953

19. Adams, C. E., N. H. Farlow, and W. R. Schell, Geochimica et Cosmuchimia, 18, 18 (1960)

20. Adams, C. E., and J. P. Wittman, The Nature of Individual Radioactive Particles from An ABD of Operation Upshot-Knothole, USNRDL-440, 1954

21. Adams, C. E., and J. D. O'Connor, The Nature of Individual Radioactive Particles. VI. Fallout Particles from a Tower Shot, Operation Redwing, USNRDL-TR-208, 1958

22. Farlow, N. H., Analyt. Chem. 29, 883 (1957)

23. Kenjiro Kimura, Geneva Conference on The Peaceful Uses of Atomic Energy, 7, 196 (1956)

24. Mackin, J., P. Zigman, D. Love, D. McDonald, and D. Sam, J. Inorg, Nucl. Chem., 15, 20 (1960)

25. Jones, J. W., and R. T. Overman, AECD-2367, 1948

26. Miller, C. F., and P. Loeb, Ionization Rate and Photon Pulse Decay of Fission Products from The Slow Neutron Fission of U-235, USNRDL-TR-247, 1958

27. Freiling, E. C., Fractionation Correlations, USNRDL-TR-385, 1959

28. Larson, K. H., J. W. Neel, et al., Summary Statement of Findings to the Distribution, Characteristics, and Biological Availability of Fallout Debris Originating from Testing Programs at the Nevada Test Site, UCLA-438, 1960

29. Nishita, Hideo, E. M. Romney, and K. H. Larson, Agricultural and Food Chemistry, 9, 2, 101 (1961)

30. Bellamy, A. W., et al., The 1948 Radiological and Biological Survey of Areas in New Mexico Affected by the First Atomic Bomb Detonation, UCLA-32, 1949.

31. Rainey, C. T., et al., Distribution and Characteristics of Fallout at Distances Greater Than Ten Miles from Ground Zero, March and April, 1953, Operation Upshot/Knothole, WT-811, 1954.

32. Lindberg, R. G., et al., The Factors Influencing the Biological Fate and Persistence of Radioactive Fallout, Operation Teapot, WT 1177, 1959.

33. Romney, R. G. Lindberg, H. A. Hawthorne, B. G. Bystrom, and K. H. Larson, Health Physics (to be published).

34. Fuller, R. K., unpublished data, USNRDL, 1960.

35. Heiman, W. T., and R. L. Stetson, unpublished data, USNRDL, 1952.

36. Miller, C. F., Analysis of Fallout Data, II. Radioactive Decay, USNRDL-TR-221, Del. 1958.

37. Dunning, Gordon M., Ed., Radioactive Contamination of Certain Areas in the Pacific Ocean from Nuclear Test Washington, D.C. Atomic Energy Commission, August 1957.

38. Lapp, Ralph E., Local Fallout Radioactivity, Bulletin Atomic Scientists, XV, 5, 181, 1958.

39. Knapp, H. A., External Gamma Doses and Dose Rates from the Fallout from Nuclear Detonations, Civil Defense, Hearings before a Subcommittee of the Committee on Government Operations, U.S. Congress. 1960.

40. Miller, J. R., and R. F. Reitemeier, Rate of Leaching through Sorts by Simulated Rain and Irrigation Waters, ARS Report No. 300, 1957.

41. Thornthwaite, C. W., J. R. Mather, and J. K. Nakamura, Science, 131, 1015 (1960).

42. Sartor, J. D., and W. L. Owens, Radiological Recovery of Land Target Components, Complex I and II, USNRDL-TR (in preparation), 1961.

Chapter 3

A THERMODYNAMIC MODEL OF FALLOUT FORMATION

3.1 The Condensation Process

The essential features of the fallout formation process deduced from the final structures, compositions, and general properties of fallout particles as described in Sections 2.3 and 2.4 are that:

1. Some portion of the radioactive elements condenses into liquid particles.

2. Some portion condenses onto the surface of solid particles.

3. If a time limit is placed on the process, some fraction of some of the radioactive elements will be still in the vapor phase.

Even in the case where the bulk carrier is sea water, the first two statements are valid for the fallout from a moderately high-yield detonation near the sea surface, since the temperature of the drops, at the altitude of the cloud, will at some time fall below freezing.

The general condensation process can be divided into two general time periods. The first period of the process is characterized by the presence of gas and liquid phases and the second period by the existence of gas and solid phases. The first period of condensation ends when the bulk carrier particles solidify. There is probably no real precise instant at which this occurs in the fireball since temperature gradients must certainly exist; the different-sizes of particles cool and solidify at different rates and times.

One most important aspect of the condensation of the radioactive fission products into the liquid phase is that the fission-product elements and compounds are dissolved to form a very dilute solution. Because of this dilution, the solution process can be treated with neglect of (a) surface saturation effects and (b) interactions among the various radioactive elements in the formation of the solution.

In a glassy matrix, i.e., after solidification, the dissolved or compounded fission products should not be able to escape. With concentrations of the order

Figure 3.5
GROSS AIR IONIZATION RATE FRACTIONATION NUMBER, r_{fp}, RELATIVE TO THE IONIZATION RATE (in hours) OF THE FISSION PRODUCTS FROM THERMAL NEUTRON FISSION OF U-235, FOR THE FISSION PRODUCT MIXTURES FROM OTHER FISSILE NUCLIDES AND NEUTRON ENERGIES

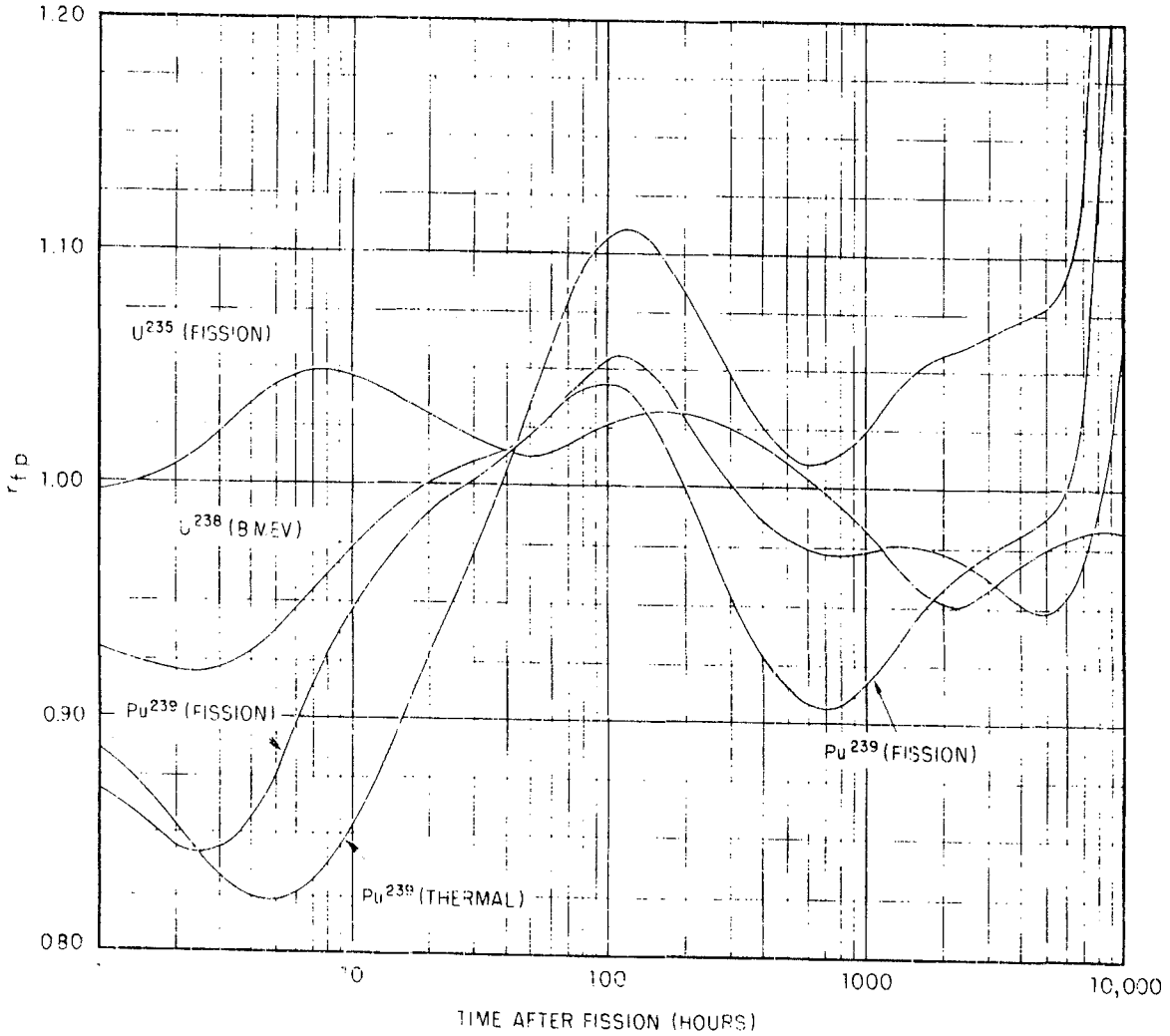

Figure 3.6
GROSS AIR IONIZATION RATE FRACTIONATION NUMBER, r_{fp}, RELATIVE TO THE IONIZATION RATE (in years) OF THE FISSION PRODUCTS FROM THERMAL NEUTRON FISSION OF U-235, FOR THE FISSION PRODUCT MIXTURES FROM OTHER FISSILE NUCLIDES AND NEUTRON ENERGIES

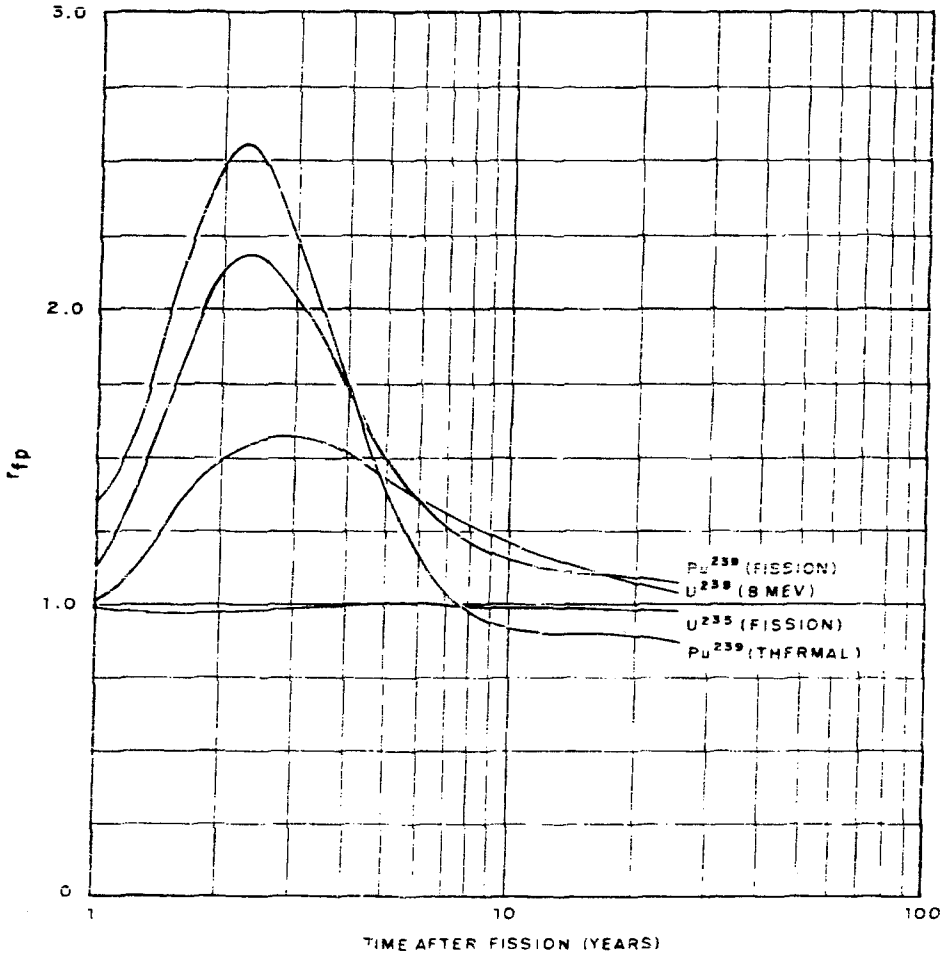

The H+1 ionization rates at 3 feet above an infinite smooth contaminated plane for a unit yield distribution of fission products per unit area are summarized in Table 3.18. The highest value is for the thermal neutron fission of U-235; the lowest is for fission-neutron fission of Pu-239.

Table 3.18

SUMMARY OF H+1 IONIZATION RATES OF NORMAL FISSION PRODUCTS[a]

Type of Fission	(H+1 Ionization Rate) / (unit yield/unit area)	
	(r/hr at 1 hr) / (fiss/sq ft)	(r/hr at 1 hr) / (KT/sq mi)
U-235 (thermal)	7.60×10^{-13}	3950
U-235 (fission)	7.58×10^{-13}	3940
U-238 (8-Mev)	6.94×10^{-13}	3610
Pu-239 (thermal)	6.70×10^{-13}	3480
Pu-239 (fission)	6.54×10^{-13}	3400

a. Per unit yield per unit area, for 3 feet above an infinite smooth contaminated plane.

The same value, 1.45×10^{23} fissions/KT, was used to convert all the ratios from fissions to kilotons. The corresponding ionization rate factor derived from ENW is (1240 r hr a 1 hr)/(KT/sq mi.) or about a factor of 3 lower than the values of Table 3.18. Other authors[15,16,17,18] have made similar calculations and comparisons of these factors and of the decay curves for the thermal neutron fission of U-235.

The number of photons per disintegration and the average energy of the photons for the normal mixture of fission products from 8-Mev-neutron fission of U-238 are shown as a function of time after fission in Figures 3.7 and 3.8, respectively.

Figure 3.7
NUMBER OF PHOTONS PER DISINTEGRATION FOR THE NORMAL MIXTURE OF FISSION PRODUCTS FROM 8-Mev NEUTRON FISSION OF U-238

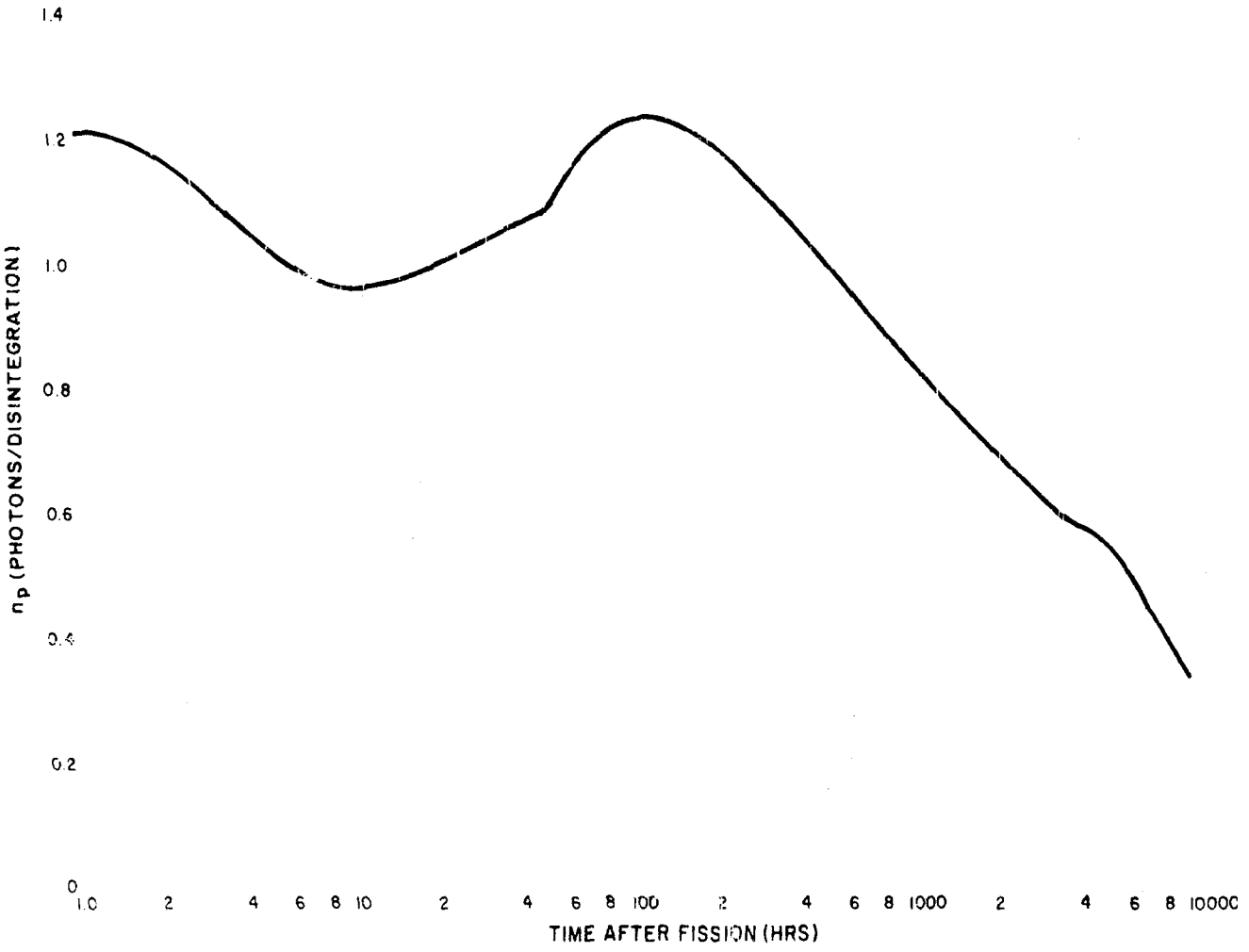

Figure 3.8
AVERAGE ENERGY OF THE PHOTONS FROM THE NORMAL MIXTURE OF FISSION PRODUCTS FROM 8-Mev NEUTRON FISSION OF U-238

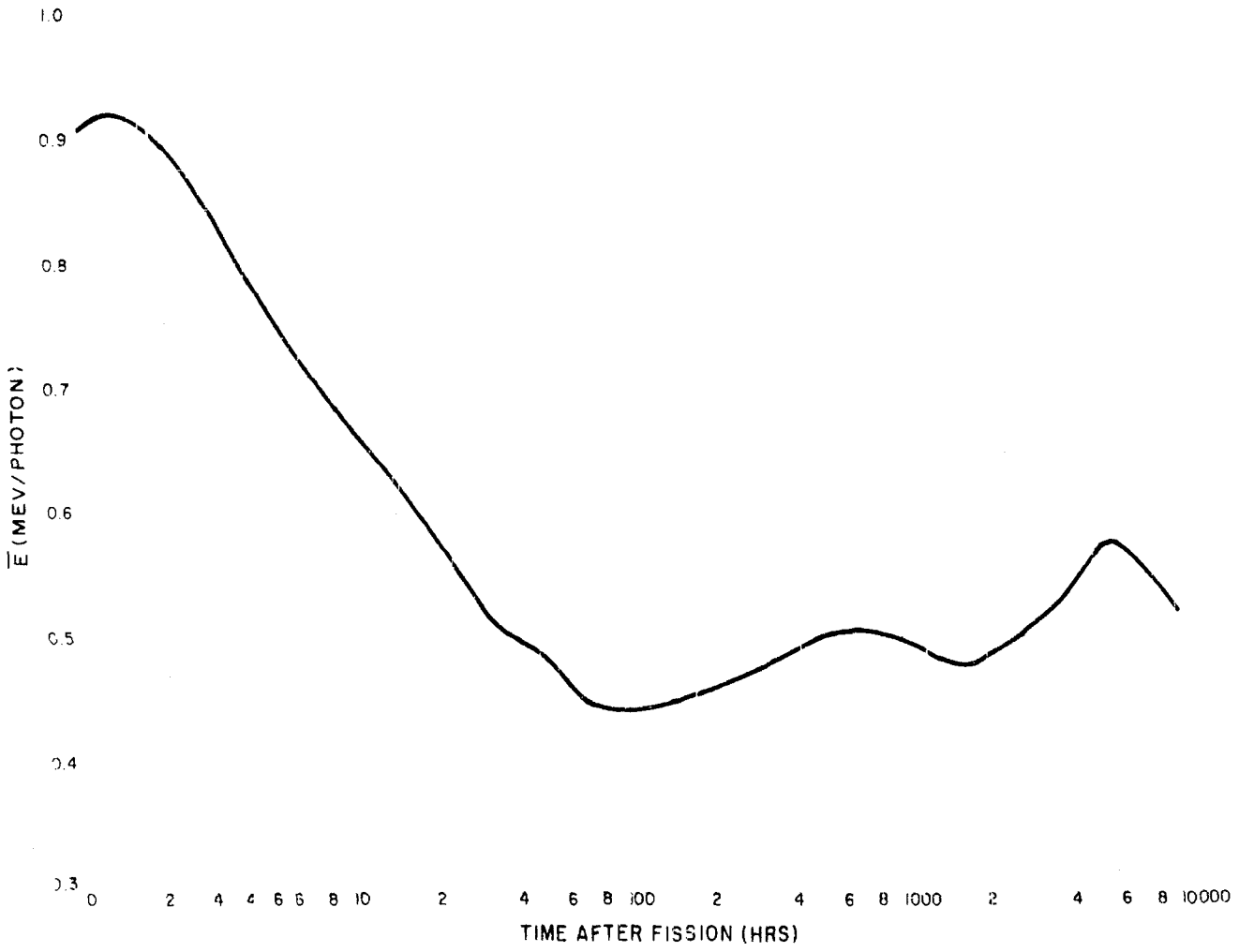

The ratio of the response of an AN/PDR-39(JIB) radiac held by a man at about 3 feet above a uniform distribution of fission products over a plane area to the calculated air ionization rate is shown in Figure 3.9 as a function of time after fission. The instrument, for the indicated response, is held by a man and is calibrated with a Co-60 standard source.[12] The ratio varies from about 73 to 77 percent; most of the reduction in the ionization rate measured is due to attenuation of the gamma rays by the person holding the instrument and by the batteries and other dense materials near the ion chamber of the instrument.

The only estimates of the ionization rate of mixed fission products at early times after fission available are those for the products of thermal neutron fission of U-235. The data, and calculations of the gamma energy release, from these fission products at early times, after fission have been summarized by Zigman and Mackin.[19] This summary of the gamma ray abundances is converted to the ionization rates, photon energy emission rate, and average photon energies given in Table 3.19. To adjust the ionization rate values calculated from the data of Zigman and Mackin to those of Table 3.17 at 45.8 minutes, the former were increased by 22.5 percent; this adjustment provides a smooth join of the ionization rate decay curve from the early to the later times.

The computed ionization rates for the fission product elements condensed in the liquid of the ideal soil when it solidifies at 1400°C (end of the first period of condensation) for times of 9 seconds (84-KT) and 60 seconds (14-MT) are given in Table 3.20 for 8-Mev neutron fission of U-238. Also given are the r_{fr} values, with respect to the normal fission-product mixture from thermal neutron fission of U-235. The variation in Figure 3.10 of the computed values of r_{fp} with time after fission shows that the dependence of the fractionation on times of condensation of 9 seconds and 60 seconds (84 KT and 14-MT, respectively) is not large, but that between about 2 hours and 4000 hours after fission the mixture from the lower yield is more highly fractionated.

The minimum in the curve at 2 hours is due to major depletions in Cs and Te, whereas the minimum at about 200 hours is due to depletions in I 131 and Ba-140 - La-140. The maximum in the curve, at 3500 hours, results from the high abundance of Zr-95 - Nb-95, and the peaks at times longer than 10,000 hours are due to the high yields of the rare earth elements from U-238 fission products with respect to the U-235 fission products.

The observed variation in r_{fp} with time after fission as measured with a standard ionization chamber, is shown in Figure 3.11 for the fallout from a low tower shot.[20] The observed r_{fp} value at 1 hour after detonation is very close to the values computed for the larger yields and with the exception of some details in the curve that may be due in part to the response characteristics of the ion chamber and, in part, to the type of fission, the calculated curves follow the trend of the observed curve quite well.

Figure 3.9
RELATIVE RESPONSE OF THE AN PDR-39(T1B) PORTABLE RADIAC HELD BY A MAN AT 3 FEET ABOVE AN EXTENDED PLANE AREA CONTAMINATED WITH FISSION PRODUCTS FROM THERMAL NEUTRON FISSION OF U-235

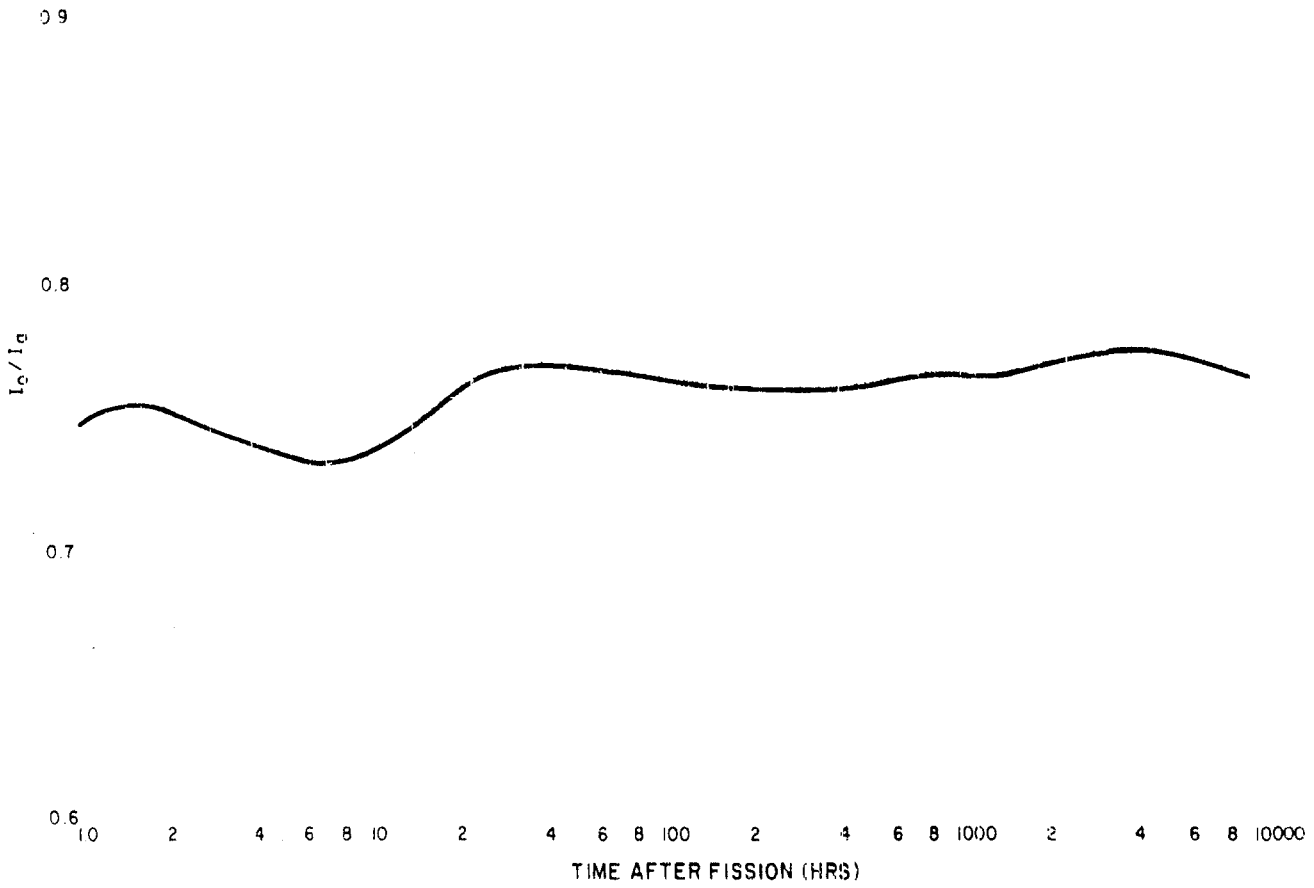

Table 3.19

EARLY-TIME IONIZATION RATE, PHOTON ENERGY EMISSION RATE, AND AVERAGE PHOTON ENERGY FOR FISSION PRODUCTS FROM THERMAL NEUTRON FISSION OF U-235

Time After Fission (secs)	Air Ionization Rate $(10^{-13}$ r/hr)/(fission/sq ft)	Photon Energy Emission Rate (Mev/sec)/(10^{4} fissions)	Average Photon Energy (Mev/photon)
1	25,600	5,020	1.150
1.5	19,800	3,940	1.178
2	16,600	3,300	1.200
3	12,700	2,530	1.235
4	10,300	2,060	1.262
6	7,530	1,510	1.296
9	2,680	1,060	1.328
13	3,820	768	1.348
19	2,680	541	1.363
28	1,840	368	1.375
41	1,250	252	1.384
60	840	168	1.390
88	560	112	1.393
129	373	74.3	1.390
189	250	49.1	1.378
277	166	32.0	1.355
406	109	20.6	1.308
595	70.2	13.5	1.245
870	45.5	8.65	1.170
1280	28.5	5.42	1.074
1870	17.9	3.28	0.992
2750	10.5	1.92	0.958
4030	6.65	1.24	0.970
5900	4.15	0.776	0.964

Figure 3.10
VARIATION OF r_{fp} WITH TIME AFTER FISSION FOR THE FRACTIONATED MIXTURE OF FISSION PRODUCTS FROM 8-Mev NEUTRON FISSION OF U-238

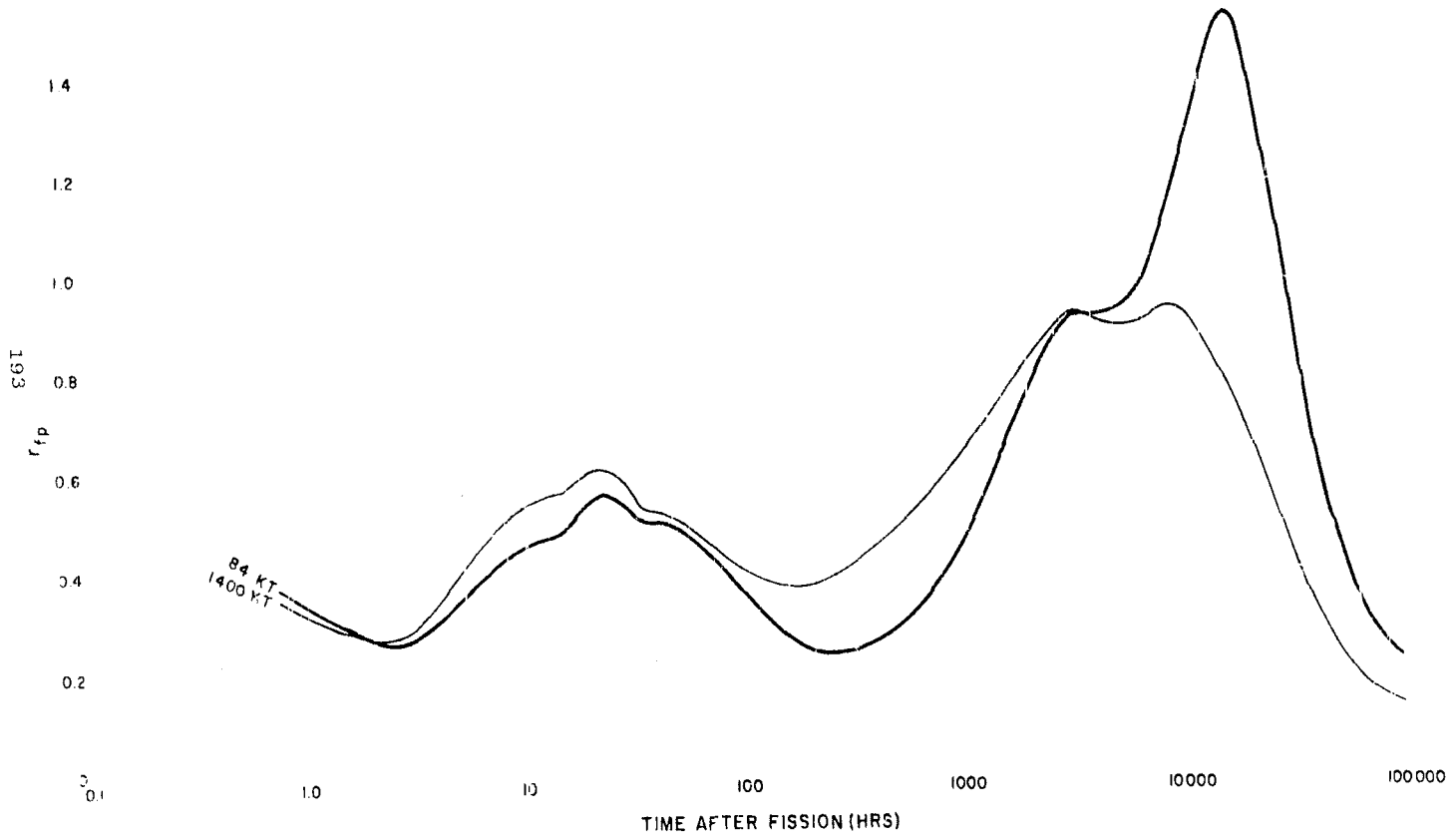

Table 3.20

IONIZATION RATE FOR FISSION PRODUCTS CONDENSED ON IDEAL SOIL AT 1400 C AT 5 SECONDS (84-KT) AND 60 SECONDS (14-MT) AFTER FISSION OF U-238 (5 MEV NEUTRONS) AND RATIO TO THAT FOR THE NORMAL MIXTURE FROM FISSION OF U-235 (THERMAL NEUTRONS)

Time After Detonation			i_{fp}[a]		r_{fp}	
Years	Days	Hours	84-KT	14-MT	84-KT	14-MT
		0.763	(8)371[b]	(8)345	0.372	0.346
		1.12	(8)210	(8)220	0.331	0.316
		1.64	(8)119	(8)118	0.287	0.284
		2.40	(9)642	(9)667	0.262	0.272
		3.52	(9)393	(9)429	0.279	0.304
		5.16	(9)274	(9)313	0.339	0.388
		7.56	(9)197	(9)231	0.412	0.483
		11.1	(9)137	(9)161	0.462	0.543
		16.2	(10)890	(9)102	0.493	0.565
		23.8	(10)544	(10)589	0.560	0.607
	1.45	34.8	(10)323	(10)337	0.512	0.535
	2.13	51.1	(10)183	(10)189	0.431	0.507
	3.12	74.9	(11)965	(10)103	0.424	0.453
	4.57	110.	(11)503	(11)591	0.339	0.398
	6.70	161.	(11)269	(11)368	0.269	0.368
	9.82	236.	(11)162	(11)259	0.239	0.382
	14.4	346.	(11)110	(11)191	0.245	0.426
	21.1	506.	(12)823	(11)141	0.283	0.485
	30.9	742.	(12)639	(11)100	0.352	0.551
	45.3	1,087.	(12)498	(12)678	0.469	0.639
	66.4	1,594.	(12)387	(12)455	0.639	0.752
	97.3	2,335.	(12)293	(12)311	0.798	0.846
	143.	3,430.	(12)198	(12)200	0.913	0.922
	208.	4,990.	(12)110	(12)107	0.921	0.896
	301.	7,220.	(13)479	(13)438	0.982	0.898
1.20	438.	10,520.	(13)170	(13)129	1.215	0.922
1.78	650.	15,600.	(14)577	(14)319	1.486	0.821
2.60	949.	22,780.	(14)279	(14)128	1.375	0.630
3.80	1,387.	33,300.	(14)133	(15)599	0.921	0.415
5.58	2,037.	48,900.	(15)575	(15)284	0.495	0.246
8.18	2,986.	71,700.	(15)292	(15)161	0.285	0.157
12.0			(15)194	(15)111	0.206	0.118
17.6			(15)135	(16)807	0.166	0.097
25.7			(16)936	(16)607	0.130	0.085

a. r/hr at 3 ft above an infinite smooth plane for 10^4 fissions per sq ft.

b. Number in parenthesis is number of decimal points between decimal point and first digit (see Figure 3.21).

Figure 3.11
OBSERVED VARIATION OF r_{fp} WITH TIME AFTER FISSION FOR CLOSE-IN FALLOUT FROM A LOW TOWER SHOT AT THE NEVADA TEST SITE

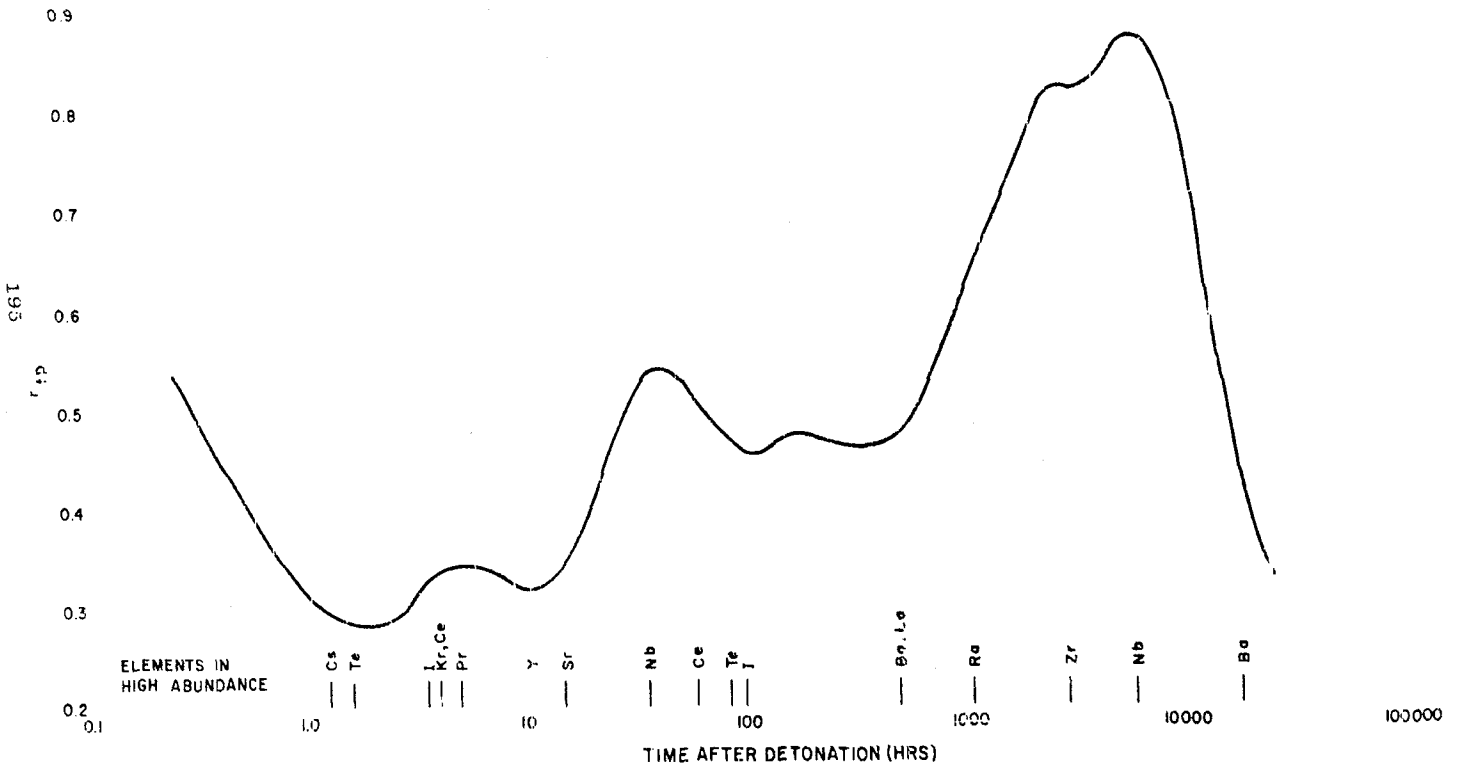

For an r_{fp} of 33 percent at H+1, the ionization rate at 1 hour per KT per sq mi. would be 1190 for the mixture of fission products condensed up to the indicated times. If the fallout also contained neutron-induced activities that contribute at H+1, the ratio would be higher. The important likely (or possible) induced activities are those produced from neutron captures by U-238 as was found by Kimura[7], Mackin[8], Freiling[22] and also reported by Stewart, Crooks and Fischer[21].

The activities and ionization rates of the possible product nuclides, for a yield of 10^4 atoms at zero time and up to 100 days later, are summarized in Tables 3.21 to 3.24. For the case in which the tabulated activities are associated with the activities from 10^4 fissions, they are equivalent to a yield of one product-nuclide for each fission. Thus, for the case where one of the neutrons from each fission event results in a (n, γ) reaction with U-238, the ionization rate from the products U-239 and Np-239 at H+1 would be 0.357×10^{-13} r/hr per fission or about 180 r/hr per KT/sq mi. The ratio for the gross mixture is then 1370 r/hr at 1 hour per KT/sq mi.

If the relative yield of U-237 was that found by Kimura[7], namely 0.15 atoms per fission, the additional activity at H+1 would be 0.0020×10^{-13} r/hr per fission or about 1 r/hr per KT/sq mi. A yield of 0.15 atoms per fission of U-240, however, would give a contribution at H+1 of about 20 r/hr per KT/sq mi. If this occurred, the ratio for the mixture would be 1390 r/hr at 1 hour per KT/sq mi. The observed ratio for this mixture of radionuclides in fallout particles on an open real terrain would be less than this value, due to both the instrument response mentioned above and to shielding by the roughness of the terrain. If it is assumed that the instrument response to the final mixture is about the same as it is for the normal mixture of fission products, then a value of about 75 percent (see Figure 2.9) would be appropriate for the AN/PDR-39(TIB) or similar radiac instrument. An effective terrain attenuation of 75 percent with respect to the ideal smooth plane would give an observed value for the ratio of about 780 r/hr at 1 hour per KT/sq mi. This is lower than the value, 1240, obtained from the data of the ENW.

Additional discussions of how the condensation process may proceed at times longer than the end of the first period of condensation, and of how the radioactive composition can vary with particle size and downwind distance, are given in Chapter 6.

Table 3.21

ACTIVITY FROM U-237 FOR 10^4 ATOMS AT ZERO TIME[a]: C(U-237) = 1

Time After Fission	A (d/s)	I_a (r/hr x 10^9)	I_o (r/hr x 10^9)	D_a (1) (r x 10^9)
1h	(1)1183[b]	(1)1339[b]	(2)957[b]	0
1.5h	(1)1181	(1)1336	(2)955	(2)660[b]
2h	(1)1178	(1)1333	(2)952	(1)138
3h	(1)1173	(1)1328	(2)948	(1)267
4h	(1)1168	(1)1322	(2)944	(1)400
6h	(1)1158	(1)1310	(2)936	(1)644
8h	(1)1148	(1)1299	(2)928	(1)922
10h	(1)1138	(1)1288	(2)920	0.1183
12h	(1)1129	(1)1278	(2)913	0.1438
15h	(1)1114	(1)1261	(2)901	0.182
18h	(1)1100	(1)1245	(2)889	0.219
24h	(1)1072	(1)1213	(2)867	0.293
1.5d	(1)1018	(1)1152	(2)831	0.436
2d	(2)968	(1)1095	(2)783	0.570
3d	(2)873	(2)988	(2)706	0.821
4d	(2)789	(2)893	(2)638	1.046
6d	(2)640	(2)724	(2)518	1.433
8d	(2)523	(2)592	(2)423	1.749
10d	(2)425	(2)481	(2)344	2.005
15d	(2)254	(2)287	(2)205	2.457
20d	(2)152	(2)172	(2)123	2.728
30d	(3)547	(3)619	(3)442	2.987
40d	(3)196	(3)221	(3)159	3.080
60d	(4)252	(4)285	(4)204	3.125
80d	(5)323	(5)365	(5)261	3.130
100d	(8)414	(4)468	(6)335	3.132

a. I_a, I_o, and $D_a(1)$ are for the distribution of 10^4 atoms per square foot over an infinite plane at zero time. I_a is in air ionization rates, I_o is in instrument response units.

b. Number in parenthesis is number of zeros between decimal point and first digit.

Table 3.22

ACTIVITY FROM U-239 FOR 10^4 ATOMS AT ZERO TIME[a]; C(U-239) = 1

Time After Fission	A (d/s)	I_a (r/hr x 10^9)	I_o (r/hr x 10^9)	$D_a(1)$ (r x 10^9)
1h	0.8365	0.3246	0.1799	0
1.5h	0.3485	0.13252	(1)749	0.1080
2h	0.1426	(1)5533	(1)317	0.1527
3h	(1)243	(2)942	(2)522	0.1775
4h	(2)413	(2)160	(3)888	0.1830
6h	(3)122	(4)473	(4)262	0.1839
8h	(5)334	(5)126	(6)718	0.1839
10h	(6)101	(7)392	(7)217	0.1839
12h				0.1839
15h				0.1839
18h				0.1839
24h				0.1839
1.5d				0.1839
2d				0.1839
3d				0.1839
4d				0.1839
6d				0.1839
8d				0.1839
10d				0.1839
15d				0.1839
20d				0.1839
30d				0.1839
40d				0.1839
60d				0.1839
80d				0.1839
100d				0.1839

a. I_a, I_o, D_a (1) are for the distribution of 10^4 atoms per square foot over an infinite plane at zero time

b. Number in parenthesis is number of zeros between decimal point and first digit.

Table 3.23

ACTIVITY FROM Np-239 FOR 10^4 ATOMS OF U-239 AT ZERO TIME[a]; C(U-239) 1

Time After Fission	A (d/s)	I_a (r/hr x 10^{9})	I_o (r/hr x 10^{9})	D_a (1) (r x 10^{9})
1h	(1)2873[b]	(1)3197[b]	(1)2270[b]	0[b]
1.5h	(1)3182	(1)3541	(1)2513	(1)168
2h	(1)3288	(1)3659	(1)2597	(1)349
3h	(1)3323	(1)3698	(1)2626	(1)714
4h	(1)3292	(1)3644	(1)2600	0.1084
6h	(1)3216	(1)3579	(1)2540	0.1808
8h	(1)3137	(1)3491	(1)2477	0.2512
10h	(1)3060	(1)3406	(1)2417	0.320
12h	(1)2984	(1)3321	(1)2357	0.387
15h	(1)2877	(1)3202	(1)2273	0.485
18h	(1)2769	(1)3081	(1)2187	0.579
24h	(1)2572	(1)2862	(1)2032	0.757
1.5d	(1)2215	(1)2465	(1)1750	1.077
2d	(1)1910	(1)2125	(1)1509	1.351
3d	(1)1419	(1)1579	(1)1121	1.791
4d	(1)1055	(1)1174	(2)833	2.122
6d	(2)583	(2)648	(2)460	2.545
8d	(2)322	(2)358	(2)254	2.787
10d	(2)178	(2)198	(2)141	2.910
15d	(3)462	(3)447	(3)318	3.032
20d	(4)911	(3)101	(4)719	3.062
30d	(5)467	(5)519	(5)369	3.067
40d	(6)240	(6)267	(6)190	3.068
60d				3.068
80d				3.068
100d				3.068

a. I_a, I_o, and D_a (1) are for the distribution of 10^4 atoms per square foot over an infinite plane at zero time.

b. Number in parenthesis is number of zeros between decimal point and first digit.

Table 3.21

ACTIVITY FROM Np-240 FOR 10^4 ATOMS OF U-240 AT ZERO TIME[a], $\sigma(U\text{-}240)$ = 1

Time After Fission	A (d/s)	I_a (r/hr[a] x 10^0)	I_o (r/hr x 10^0)	$D_a(1)$ (r x 10^0)
1h	0.1307	0.2765	0.2097	0
1.5h	0.1279	0.2647	0.2052	0.134
2h	0.1248	0.2583	0.2002	0.265
3h	0.1189	0.2461	0.1907	0.518
4h	0.1131	0.2341	0.1815	0.758
6h	0.1026	0.2124	0.1645	1.212
8h	(1)928[b]	0.1921	0.1489	1.611
10h	(1)843	0.1744	0.1352	1.978
12h	(1)763	0.1579	0.1224	2.312
15h	(1)658	0.1362	0.1055	2.754
18h	(1)569	0.1177	(1)913[b]	3.136
24h	(1)424	(1)878[b]	(1)680	3.750
1.5d	(1)235	(1)486	(1)377	4.547
2d	(1)130	(1)269	(1)209	4.986
3d	(2)400	(2)828	(2)642	5.372
4d	(2)123	(2)254	(2)197	5.484
6d	(3)116	(3)240	(3)186	5.530
8d	(4)110	(4)227	(4)176	5.536
10d	(5)104	(5)215	(5)167	5.538
15d	(8)286	(8)592	(8)459	5.536
20d				5.538
30d				5.538
40d				5.538
60d				5.538
80d				5.538
100d				5.538

a. I_a, I_o, and $D_a(1)$ are for the distribution of 10^4 atoms per square foot over an infinite plane at zero time.

b. Number in parenthesis is number of zeros between decimal point and first digit.

CHAPTER 3 REFERENCES

1. Stewart, K., Trans. Faraday Soc., 52, 161 (1956).

2. Kelley, K. K., Contributions to the Data on Theoretical Metallurgy, XIII. High Temperature Heat-Content, Heat-Capacity, and Entropy Data for the Elements and Inorganic Compounds, U.S. Bureau of Mines, Bulletin 584, 1960.

3. Stull, D. R., and G. C. Sinke, The Thermodynamic Properties of the Elements, Am. Chem. Soc., Washington, D.C., 1956.

4. Lapple, C. E., Fallout Control, Stanford Research Institute, SRIA-3, 1958.

5. Adams, C. E., N. H. Farlow, W. R. Schell, The Compositions, Structures, and Origins of Radioactive Fallout Particles, USNRDL-TR 209, 1958.

6. Miller, C. F., Analysis of Fallout Data, I. The Jangle "S" and "U" Shot Fallout Patterns, USNRDL-TR-220, Del. 1958.

7. Kimura, Kenjiro, Geneva Conference on the Peaceful Uses of Atomic Energy, 7, 196 (1956).

8. Mackin, J., P. Zigman, D. Love, D. McDonald, and D. Sam, J. Inorg, Nucl. Chem., 15, 20 (1960).

9. Coughlin, J. P., U.S. Bureau of Mines, Bulletin 542, 1954.

10. Bolles, R. C., and N. E. Ballou, Calculated Abundances of U 235 Fission Products, USNRDL-456, 1956.

11. Kateoff, Seymour, Nucleonics, 16, 4, 78 (1958).

12. Miller, C. F., and P. Loeb, Ionization Rate and Photon Pulse Decay of Fission Products from the Slow Neutron Fission of U-235, USNRDL-TR-247, 1958.

13. Dolan, P. T., Calculated Abundances and Activities of the High Energy Neutron Fission of Uranium-238, DASA-525, 1959.

14. Dolan, P. T., Gamma Spectra of Uranium-238 Fission Products at Various Times after Fission, DASA-526, 1959.

15. Knapp, H. A., Civil Defense Hearings before a Subcommittee of the Committee on Government Operations. U.S. Congress, External Gamma Doses and Dose Rates from the Fallout from Nuclear Detonations. 1960.

16. Lapp, Ralph E., Local Fallout Radioactivity, Bulletin Atomic Scientists. XV, 5, 181, 1959.

17. Perkins, J. F., and R. W. King, Energy Release from the Decay of Fission Products, Nuclear Sci. and Eng., 3, 726, 1961.

18. Knabe, W. E., and G. E. Putnam, The Activity of the Fission Products of U-235, General Electric Co., APEX-448, 1958.

19. Zigman, P., and J. Mackin, Early Time Decay of Fission Products, Health Physics, 5, 79, 1961.

20. Strope, W. E., Evaluation of Countermeasure System Components and Operational Plumbbob, WT-1464, 1958.

21. Stewart, N. G., R. N. Crooks, E. M. R. Fischer, Hearings of the Joint Committee on Atomic Energy, U.S. Congress, The Nature of Radioactive Fallout and Its Effects on Man, p.1690, June 1957.

22. Freiling, E. C., Fractionation Correlations, USNRDL-TR-385, 1959.

Figure 5.3
IDEALIZED FALLOUT PATTERN FOR A 1-MT YIELD SURFACE BURST FOR A WIND SPEED OF 15 MPH AND 100 PERCENT FISSION

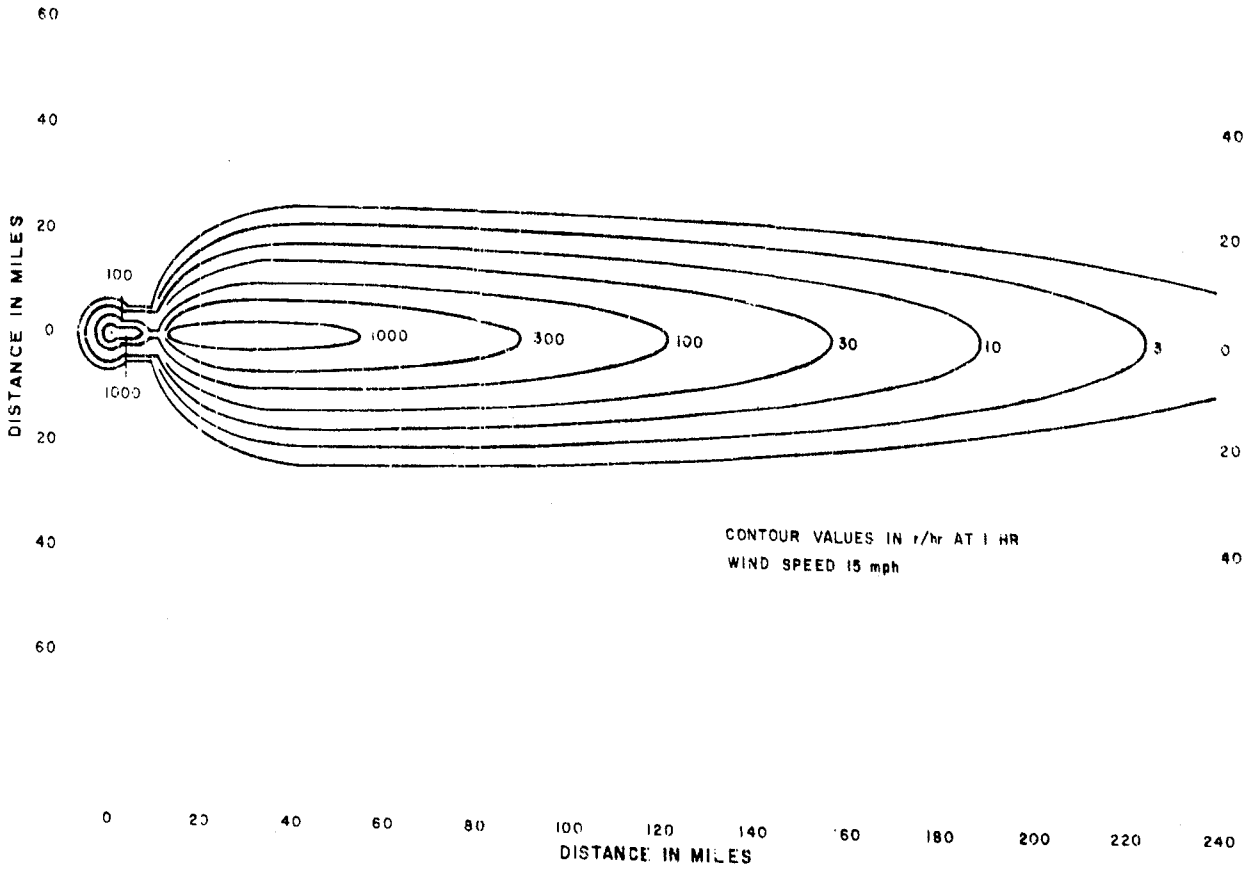

Figure 5.9
VARIATION OF IONIZATION RATE WITH TIME AFTER DETONATION AT
X = 1.87 × 10^5 FT FOR W = 10^3 KT AND A WIND SPEED OF 15 MPH

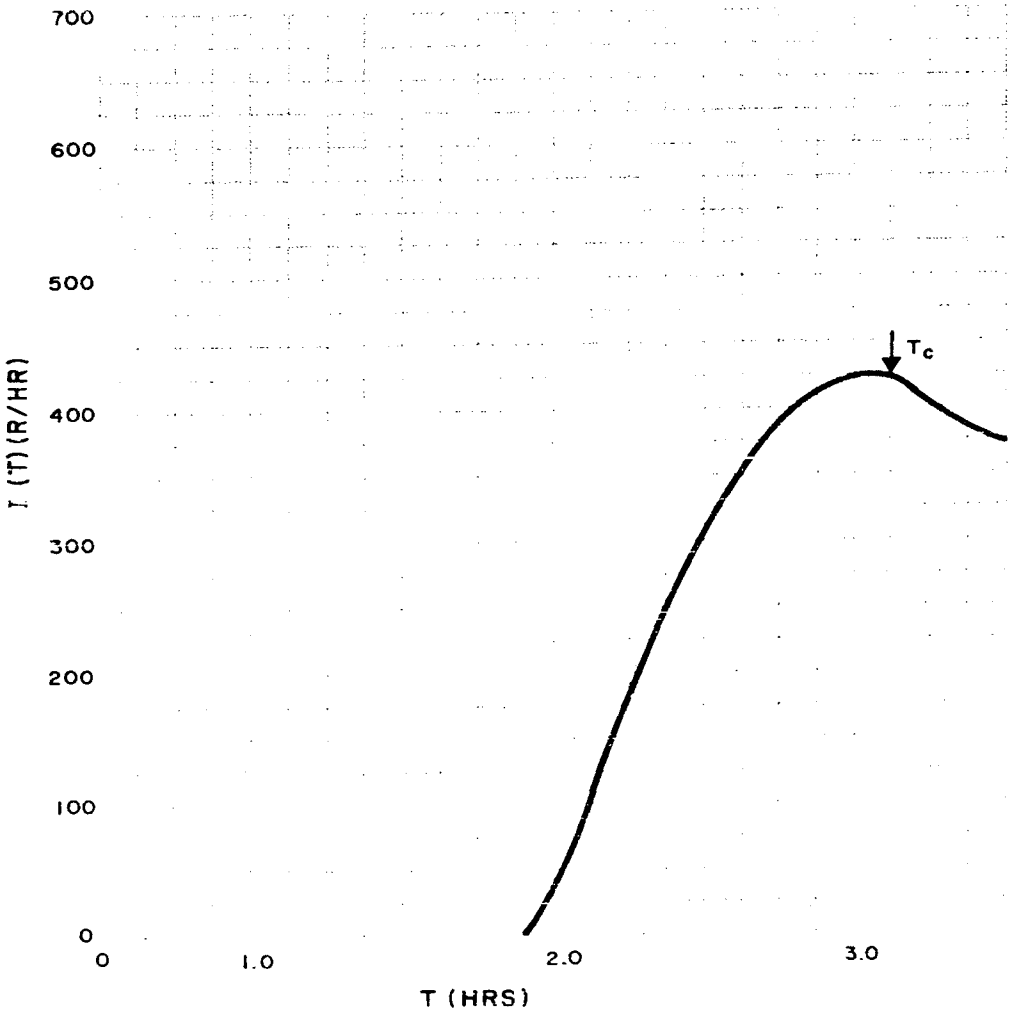

Figure 5.12
VARIATION OF THE IONIZATION RATE WITH TIME AFTER DETONATION AT
X = 3.35 × 10^4 FT FOR W = 10^3 KT AND A WIND SPEED OF 15 MPH

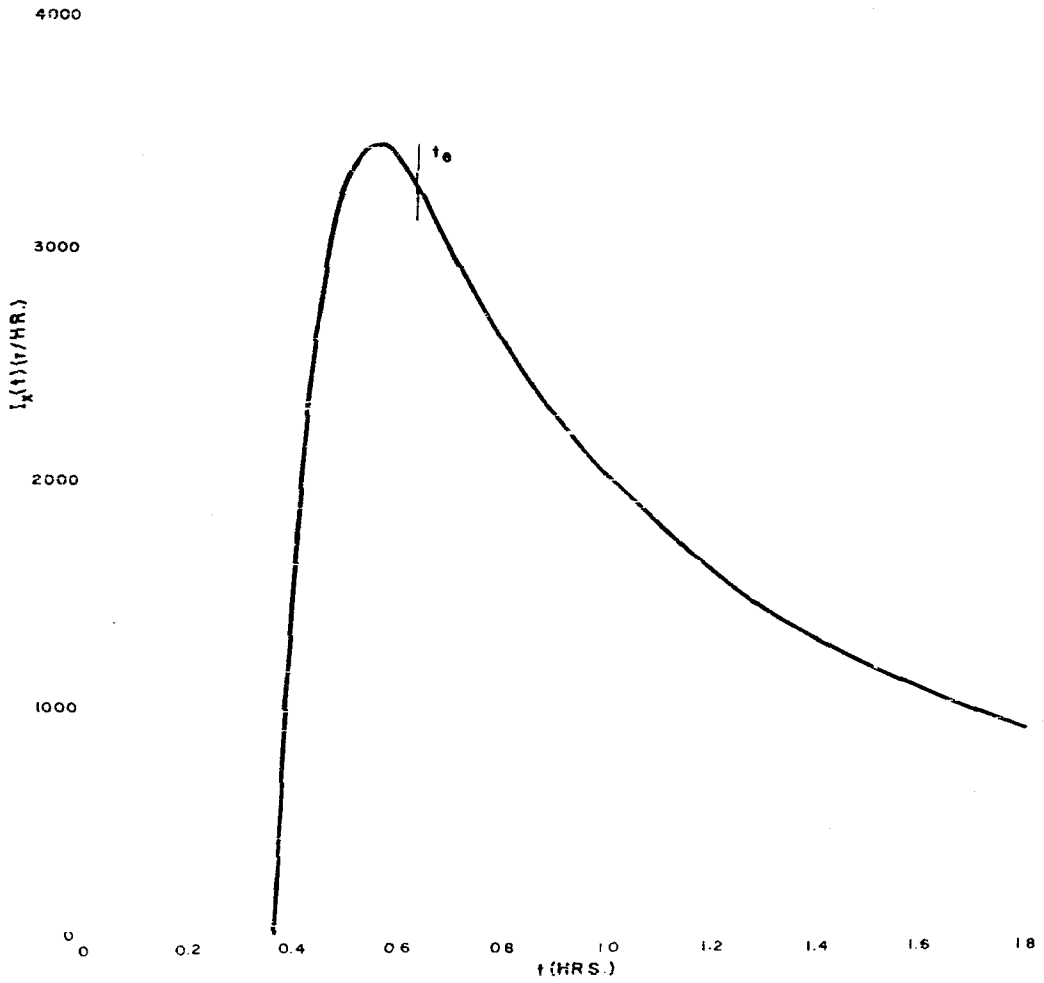

Figure 5.14
ACCUMULATED ACTIVITY DISTRIBUTION AS A FUNCTION OF PARTICLE SIZE AT X = 3.35 · 10^4 FT AND 1.87 · 10^5 FT DOWNWIND FROM THE 1-MT YIELD SURFACE BURST FOR A WIND SPEED OF 15 MPH

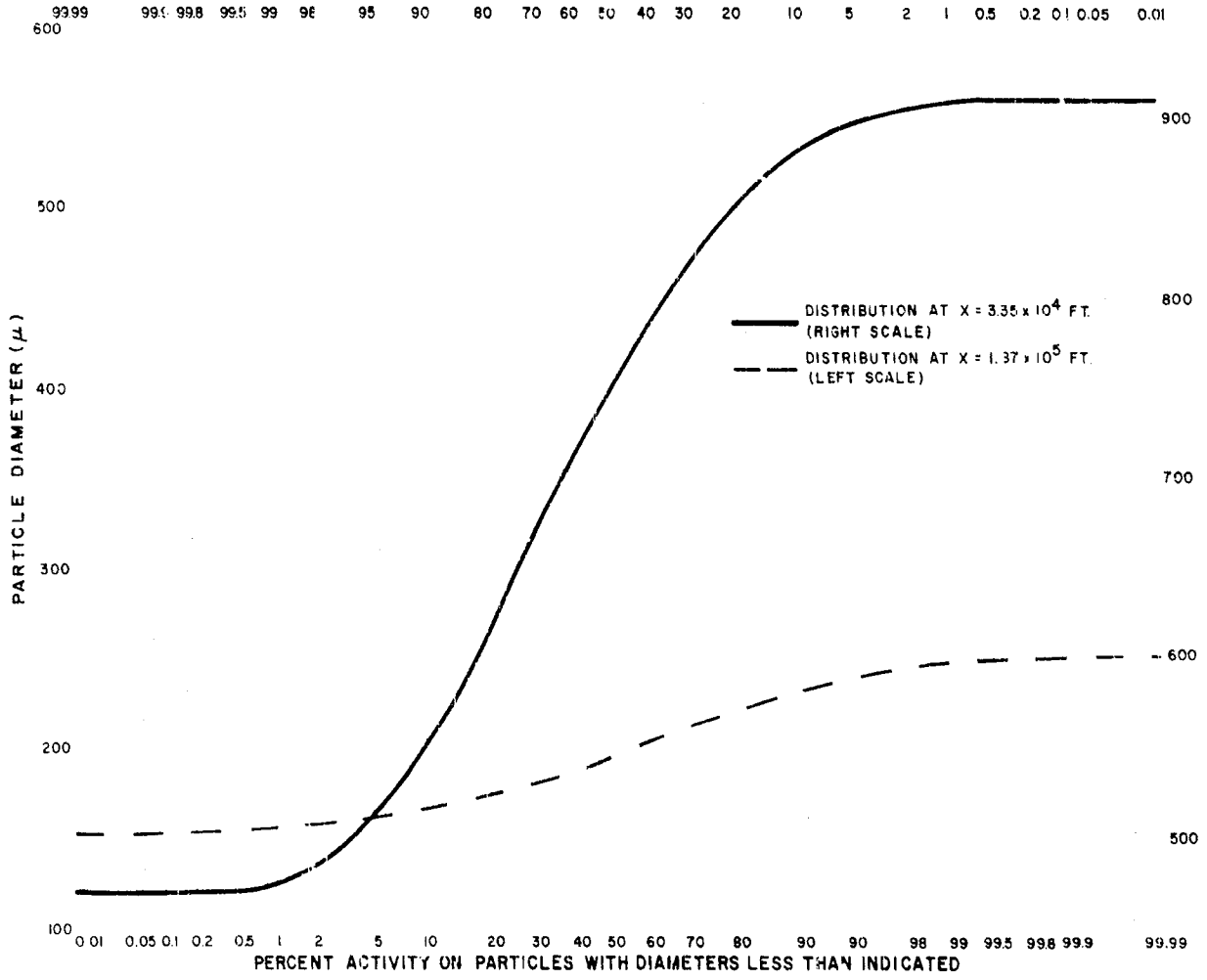

Figure 5.15
COMPARISON OF THE GROSS ACTIVITY DISTRIBUTION ON PARTICLES OF VARIOUS DIAMETERS DERIVED FROM THE SIMPLIFIED FALLOUT SCALING SYSTEM TO DISTRIBUTIONS USED IN OTHER MATHEMATICAL FALLOUT MODELS

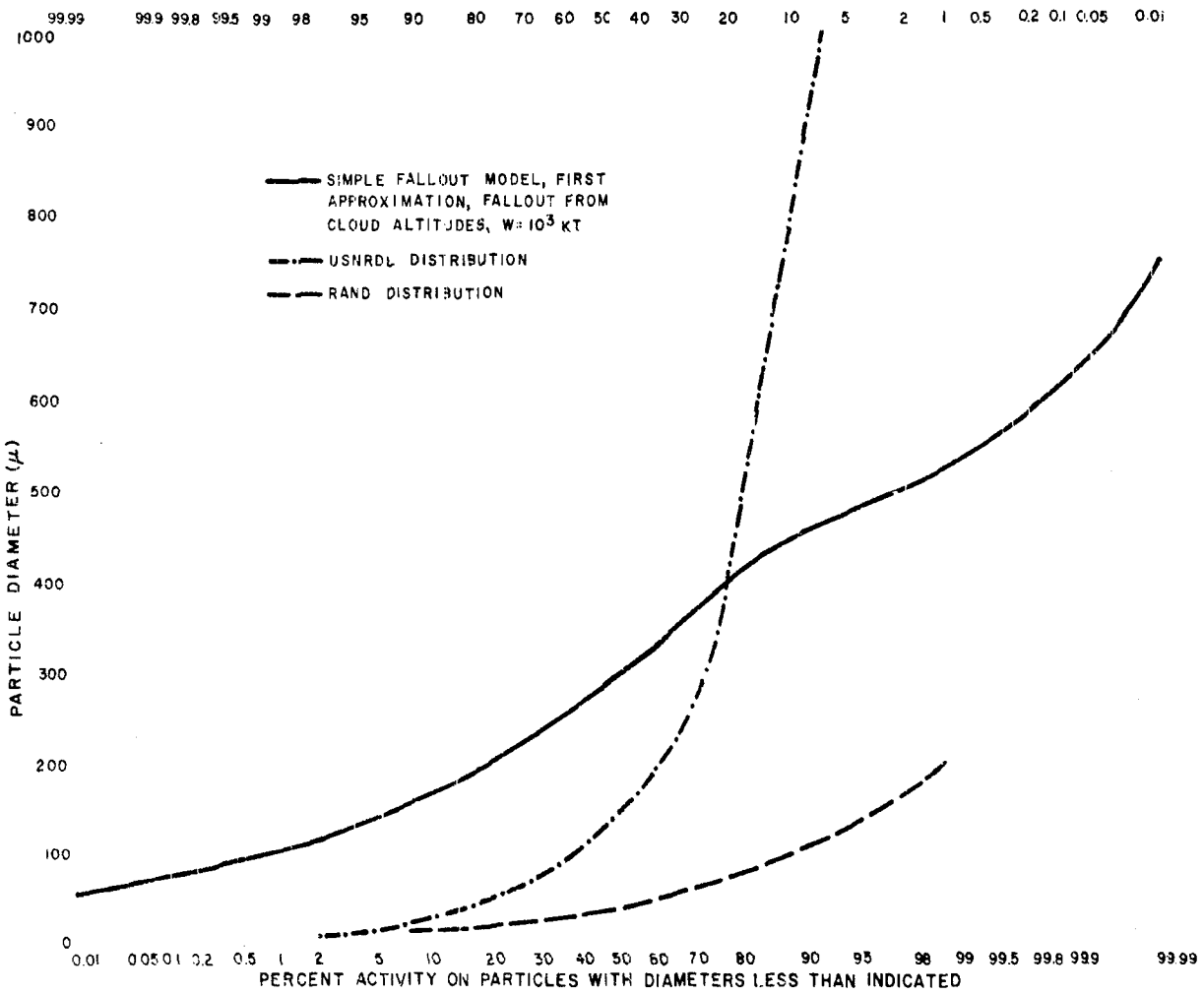

Table 5.10

WIND DATA AND PARTICLE FALL TRAJECTORY COMPONENTS FOR JANGLE "S" SHOT

Altitude increment (10^3 ft)	Wind Direction (degrees)	Wind Speed (knots)	$\Delta\theta$ (degrees)	10^{-5} knot/ft				
				$v_f \Delta d$	$v_f \Delta y$	$v_f \Delta x$	$v_f \Sigma y$	$v_f \Sigma \Delta x$
11-12	200	37	0	37	0	37.00	22.23	186.04
10-11	200	34.5	0	34.5	0	34.50	22.23	149.04
9-10	200	32	0	32	0	32.00	22.23	114.54
8-9	200	28	0	28	0	28.00	22.23	82.54
7-8	180	26	20	26	8.89	24.44	22.23	54.54
6-7	180	20	20	20	6.84	18.80	13.34	30.06
5-6	170	13	30	13	6.50	11.26	6.50	11.26
4[a]-5	calm	calm	--	0	0	0	0	0

Note: Cloud base at ~ 10 minutes: $h_b \sim$ 9,000 ft.
Cloud top at ~ 10 minutes $h_t \sim$ 12,000 ft.

a. Surface (4,200 ft).

Figure 5.16
PLOT OF PARTICLE FALL TRAJECTORY COMPONENTS RELATIVE TO ESTIMATED PATTERN CENTER LINE FOR CASTLE BRAVO WINDS

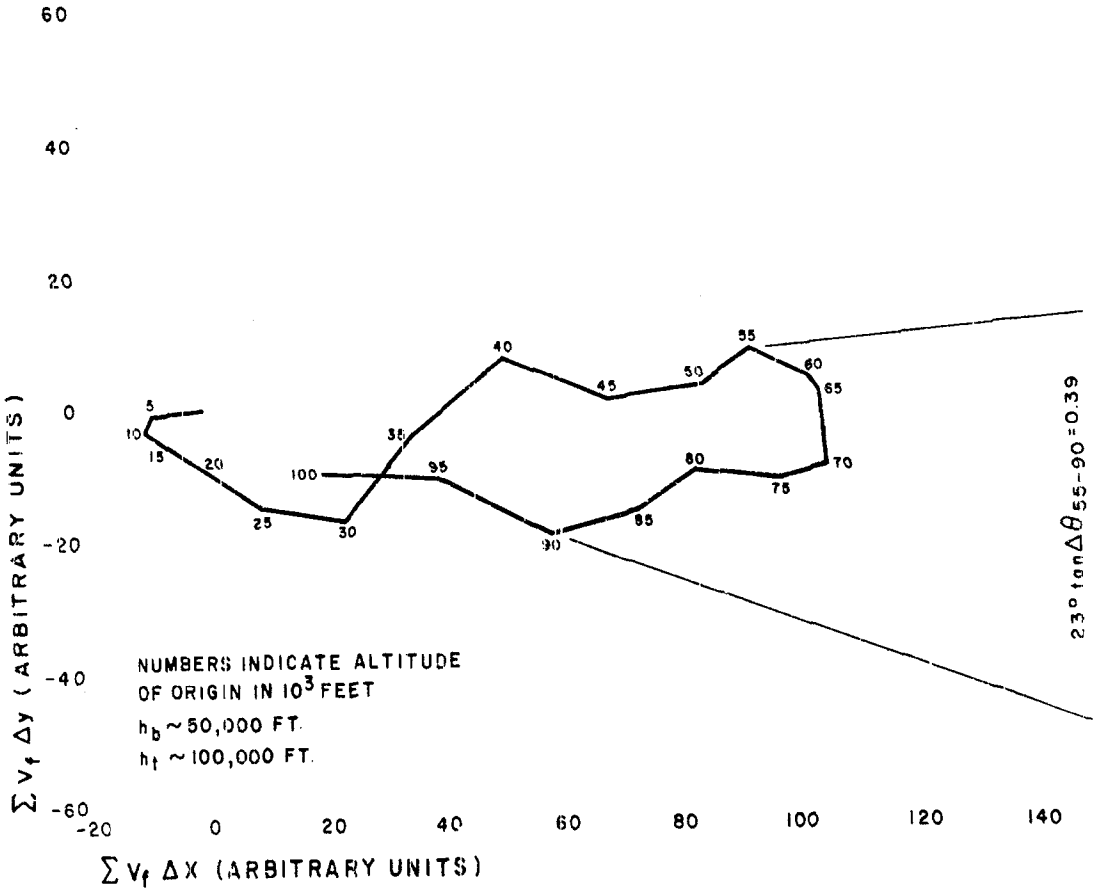

Figure 5.17
VARIATION OF THE CALCULATED INFINITE IDEAL PLANE STANDARD INTENSITY WITH DOWNWIND DISTANCE (Center Line of Pattern) FOR A 10-MT YIELD SURFACE DETONATION (100% Fission)

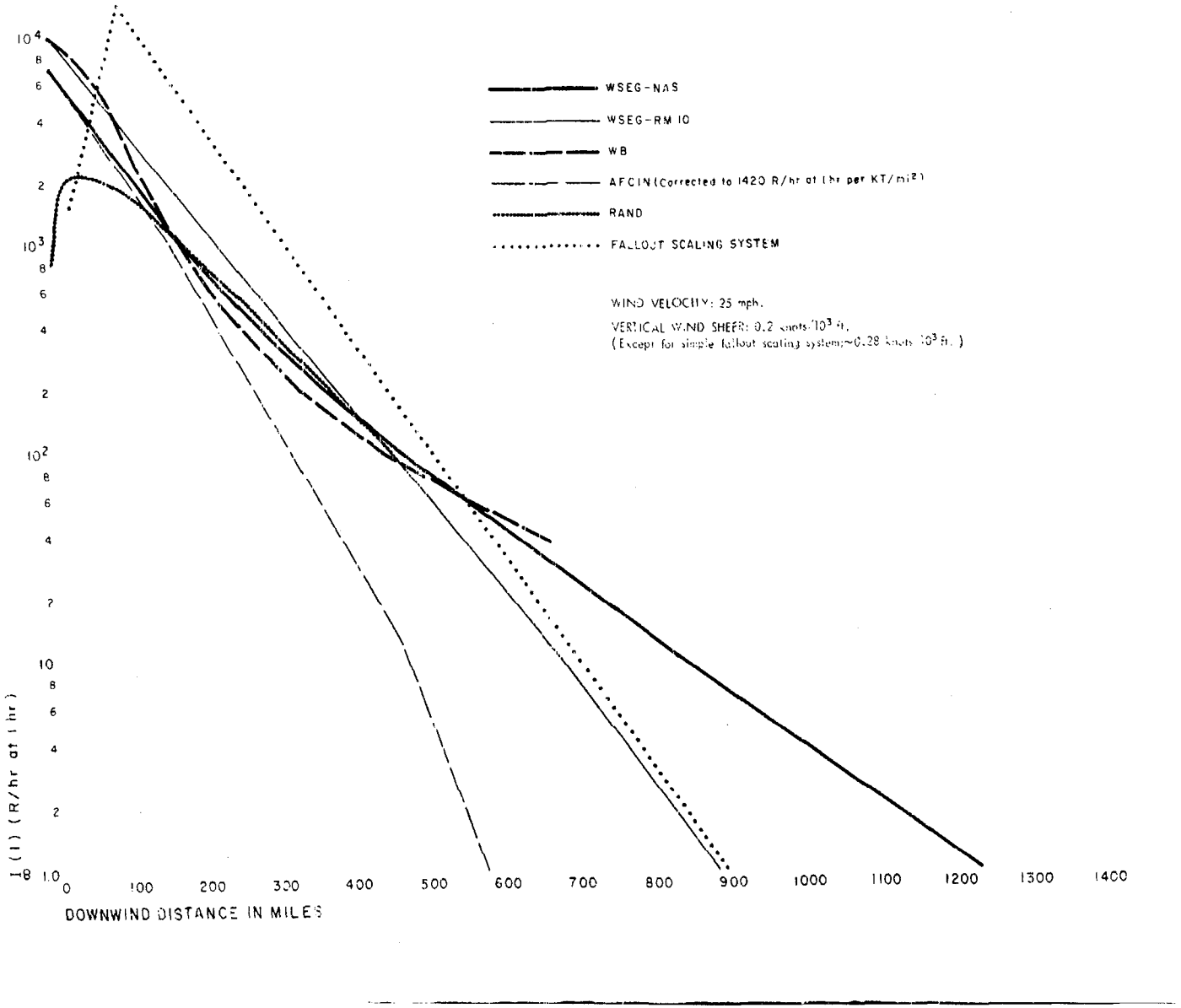

CHAPTER 5 REFERENCES

1. LaRiviere, P.D., Early-Time Gamma Ray Properties of U-235 Gross Fission Products, USNRDL-TM-89, 1958.

2. Clark, D.E., and A.D. Anderson, Private communication, USNRDL, July 1960.

3. Pugh, G.E., and R.J. Galiano, An Analytic Model of Close-In Deposition of Fallout for Use In Operational-Type Studies.

4. Research Memorandum No. 10, Weapons Systems Evaluations Group, 1959.

5. Ferber, Gilbert J., and Jerome L. Heffter, A Comparison of Fallout Model Predictions With a Consideration of Wind Effects, U.S. Weather Bureau, 1961.

6. Batten, E.S., D.L. Ingleheart, and R.R. Rapp, Derivation of Two Simple Methods for the Computing of Radioactive Fallout, RM-2560, 1960.

7. Nagler, K.M., L. Machta, and F. Pooler, Jr., A Method of Fallout Prediction for Tower Bursts at the Nevada Test Site, TID-5489, OTS, Department of Commerce, Washington 25 D.C., 1955.

8. U.S. Government, Nuclear Weapons Employment Handbook, Air Force Manual 200-8, 1961 (Classified).

9. The Effects of Nuclear Weapons, U.S. Government Printing Office, Washington D.C., 1957.

10. Anderson, A.D., Scaling Relations for Fallout Dose-Rate Patterns from Land Surface Nuclear Bursts, USNRDL-TR (in publication, 1961).

The fraction-of-device contour ratio, in terms of the total number of fission events, is

$$FD_r(1) = \frac{7.1\times10^{-24}}{D(1)q_x BW\left[r_\alpha(1)i_{fp}(i) + i_f(1)\right]} \text{ (r/hr at 1 hr-sq ft)}^{-1} \qquad (6.41)$$

or, for the standard values of D(1), q_x, and $i_f(1)$,

$$FD_r(1) = \frac{1.83\times10^{-11}}{BW\left[r_\alpha(1) + 0.019\right]} \qquad (6.42)$$

The fraction-of-device contour ratio has two uses. The first is that it is used to estimate the surface density of constituents that are assumed to mix uniformly with the more refractory fission products. The second is that it is used in conjunction with observed fallout patterns when the latter are integrated for the total fraction of the weapon contained within a stated ionization rate contour. The use of both contour ratios is illustrated in Chapter 7, Volume II.

For a land surface burst, the average concentration of the fission products is estimated from the ratio of FP_r (1) to M_r (1); this is

$$C_{fp} = \frac{3.32\times10^{-24}BW^{0.083}\Sigma_{jA}r_{jA}(\alpha)}{f(\alpha)} \quad \frac{\text{moles fp}}{\text{mg fallout}} \qquad (6.43)$$

6.4 Foliage-Contamination Factor Contour Ratio

In Chapter 2, the foliage contamination factor, a_L, was defined as the ratio of the number of fissions in the fallout on foliage per gram of dry plant (or foliage) to the number of fissions in the total deposited fallout, per sq ft of soil. Also, the foliage surface density, w_L, (subject to contamination) was defined as the grams of dry foliage per sq ft of soil. Therefore, the foliage-contamination factor contour ratio is defined by

$$FC_r(t) = \frac{a_f w_L}{K_\alpha(t)} \quad \frac{\text{fissions on foliage/ft}^2 \text{ of soil area}}{\text{r/hr}} \qquad (6.44)$$

The contour ratio, evaluated as of H + 1, is

$$FC_r(1) = \frac{a_L w_L}{K_\alpha(1)} \quad \frac{\text{fissions on foliage/ft}^2 \text{ of soil area}}{\text{r/hr at 1 hr}} \tag{6.45}$$

where

$$K_\alpha(1) = 3.90 \times 10^{-13} \left[r_\alpha(1) + 0.019 \right] \quad \frac{\text{r/hr at 1 hr}}{\text{fission/ft}^2} \tag{6.46}$$

when the standard values of D(1) and q_x are used. It is seen that multiplication of FC_r (1) by I(1) gives the number of fissions on foliage per sq ft of soil area.

The "zero-time" number of atoms of a given radionuclide (at least for the end member of a mass chain) in the fallout is given by

$$N_A^0 = Y_A \, FC_r(1) I(1) \quad \frac{\text{atoms on foliage}}{\text{ft}^2 \text{ of soil area}} \tag{6.47}$$

in which Y_A is the mass chain yield in atoms per fission of mass number A.

The major interest in the contamination of foliage by fallout is related to the fact that the consumption of the foliage by animals and humans may produce an internal radiological hazard. Therefore, generalization and extensions of the foliage contamination factor data from tower-and balloon-detonation fallout are needed for making estimates of the potential biological availability of the radionuclides in the fallout from other types of nuclear explosions and for various foliage contamination conditions.

When contaminated foliage is consumed, some of the radionuclides or some fraction of each nuclide ingested is dissolved in the stomach fluids; the remainder stays with the particles and pass through the digestive tract. Many of the dissolved nuclides are assimilated into the blood and concentrate in specific body organs. The factors involved in this distribution and the methods for estimating the resulting internal doses are given by K.Z. Morgan and others.[5]

However, methods are needed for estimating the relative amount of each nuclide that is soluble in the stomach fluids. Evaluations of the internal hazard can be made (for fallout conditions in a nuclear war, for example) from the generalizations of the foliage contamination factor together with estimates of the solubilities of the radionuclides.

The amount of radioactive nuclides that pass through the digestive tract may be considered separately because a large fraction of certain radionuclides in the fallout will be insoluble. For these radionuclides, only the gross amounts passing through need be considered. However, for the case of the assimilation of the soluble nuclides in other body organs, each radionuclide must be considered separately.

6.4.1 Insoluble-Nuclide Fractions

A gross estimate of the radioactivity of insoluble nuclides passing through the digestive tract from ingestion of contaminated foliage can be made if it is assumed that the gross solubility of the radioactivity is the same in the stomach as it is in 0.1N HCL. If the soluble fraction of the gross activity is defined as S(t), the number of moles of fission product atoms ingested that pass through the digestive tract with the particles is given by

$$FP_g = 3.32\times10^{-24}\left[1 - S(t)\right] A_F C_e(t) \quad \frac{\text{moles of fission products}}{\text{day}} \tag{6.48}$$

where A_F is $FC_r(t)I(t)$ in fissions on foliage/ft^2 of soil area, and $C_e(t)$ is in ft^2 of foliage consumed/day. Equation 6.48 can be written in terms of dis/sec, as

$$FP_g = \left[1 - S(t)\right] A_F C_e(t) a_{fp}(t) \quad \frac{\text{dis/sec}}{\text{day}} \tag{6.49}$$

where $a_{f_p}(t)$ is in dis/sec per fission at the time, t, after detonation. It may be noted that if $C_e(t)$ is defined in terms of grams of dry foliage per day, w_L may be eliminated from the definition of $FC_r(t)$ in Eqs. 6.44 and 6.45.

Theoretical estimates of the fractional amount of insoluble activities may be made from the data of Chapter 4 if it is assumed that all the fission-product nuclides on the exterior surface of the particles dissolve in the stomach fluids. The fraction not dissolved is then given by the $r_o(A)$ values for each of the fission-product nuclides. If these fractionation numbers are redefined as r_{jA}, where j designates the element and A the mass number (isotope), then Eqs. 6.48 and 6.49 can be written as

$$FP_g = A_F C_e(t) \Sigma_{jA} r_{jA} N_{jA}(t) \quad \frac{\text{moles of fission products}}{\text{day}} \tag{6.50}$$

and

$$FP_g = A_F C_e(t) \Sigma_{jA} r_{jA} a_{jA}(t) \quad \frac{dis/sec}{day} \tag{6.51}$$

where N_{jA} (A) is the number of atoms of element j with the mass number A per fission at the time, t, after fission, and a_{jA} (t) is the activity in dis/sec per fission of the nuclide (the indices A and j define the nuclide in terms of its mass number and its atomic number, or elemental designation).

6.4.2 Soluble-Nuclide Fractions

The solubility in digestive fluids of each element, radionuclide, carried by the fallout particles deposited on edible foliage must be known before estimates of the amounts of each that concentrate in the tissue of (specific) body organs can be made. If the nuclide solubilities in 0.1 normal HCl solution are the same as in digestive fluids, then measurements of the solubilities in the acid can be used in such estimates. If the solubility in the 0.1 normal HCl solution is defined as S_j for the jth element, the amount and radioactivity of the ith radionuclide (of element j) dissolved is

$$N^*_{jA} = 1.66 \times 10^{-24} A_F C_e(t) S_j N_{jA}(t) \quad moles/day \tag{6.52}$$

and

$$a^*_{jA} = A_F C_e(t) S_j a_{jA}(t) \quad \frac{dis/sec}{day} \tag{6.53}$$

in which S_j is the fraction of element j that is soluble. Theoretical upper-limit values of N^*_{jA} (t) and a^*_{jA} can be estimated by substituting the appropriate values of r'_o (A), redefined as r'_{jA}, given by Eq. 6.9 for S_j.

It should be emphasized that, for general applicability, the values of S(t) and S_j must be known as a function of particle-diameter. For the smaller particles, the values of R_o (A), or r_{jA}, are independent of particle size but the values of r'_o (A), or r'_{jA}, are not.

6.4.3 Variation of the Foliage-Contamination Factor with Particle Size

The values of a_L and K_α(t) depend on particle size. The dependence of the latter on the particle-size designator, α, is represented by Eq. 6.46. The dependence of a_L on α was derived from the data of Romney and coworkers[6] presented in Chapter 2.

The values of α that are applicable to the various measured values of a_L were calculated from

$$\alpha_o \quad X/h \tag{6.54}$$

where X is the distance from ground zero and h is the mid-height of the cloud. The values of α_o can be used to estimate the median particle-diameter of the particles deposited at the distance X by the methods described in Chapter 5. When v_f (the fall velocity) can be determined for the median particle diameter, as obtained from particle-size data, then the 15 mph value of α_o can be determined from

$$a_o = 22.0/v_f \tag{6.55}$$

for v_f in feet per second. The values of h and other data, for the detonations for which values of a_L are available, are given in Table 6.9.

Table 6.9

SUMMARY OF SHOT CONDITIONS FOR ESTIMATING THE MEDIAN PARTICLE DIAMETER DESIGNATOR

Shot	Yield (KT)	Height of Burst (feet)	h (feet)	Type of Shot
Tesla	7	300	24,000	Tower
Apple I	14	500	27,000	Tower
Met	22	400	35,500	Tower
Apple II	29	500	38,500	Tower
Priscilla	37	700	34,500	Balloon
Diablo	17	500	26,000	Tower
Shasta	17	500	24,000	Tower
Smoky	44	700	32,000	Tower

The values of the median particle size, with respect to the distribution of activity on the particles, for two locations each on Shots Apple II and Smoky, along with the computations of α_o, are given in Table 6.10. The α_o values calculated by the two methods are nearly the same.

Table 6.10

CALCULATION OF α_o FOR SOME FALLOUT LOCATIONS FROM SHOTS APPLE II AND SMOKY

Shot	X (miles)	d_m (microns)	v_f (ft/sec)	α_o X/h	α_o 22.0/v_f
Apple II	7	-	-	0.960	(0.960)
	48	126	3.24	6.58	6.59
	106	70	1.39	14.5	15.8
Smoky	132	56	0.94	21.8	23.4
	206	47	0.67	34.0	32.8
	259	-	-	42.8	(41.3)

The values of a_L given in Table 2.18 (see Chapter 2) are plotted in Figure 6.6 as a function of α_o values computed by use of Eq. 6.54. This set of data for the retention of fallout by native plants, is widely scattered; however, the general trend of the values of a_L from individual shots is to increase with increasing α_o. Part of the difference in the observed variation of a_L with α from one detonation to another is undoubtedly due to the fact that differences in wind speed occurred. Other causes of the differences in the variation with α could be due to differences in humidity conditions and in the predominant types of foliage that were collected for analyses.

The values of a_L calculated from the data of Table 2.16 (see Chapter 2) for the forage crops (clover, alfalfa, wheat, and mixed grasses) are plotted in Figure 6.6 as a function of the α_o values that were corrected to an average wind speed of 15 miles per hour (see Table 6.10). Since the absolute accuracy of the source data is probably not better than 50 percent, a single line was drawn through the plotted data, neglecting one point. The suggested representation of a_L for these four forage crops is therefore given by

$$a_L = 9.5\times10^{-5}\,(\alpha_o - 0.34);\ \alpha_o \geq 0.34 \qquad (6.56)$$

The complete representation of the foliage contamination factor contour ratio for evaluation at H+1 hour is then

$$FC_r(1) = \frac{2.44\times10^{8} w_L\,(\alpha_o - 0.34)}{(r_\alpha(1) + 0.019)};\ \alpha_o \geq 0.34 \qquad (6.57)$$

The value of FC_r (1) for α_o values less than 0.34 is taken to be zero.

Figure 6.6
VARIATION OF α_L WITH CALCULATED VALUES OF α_0

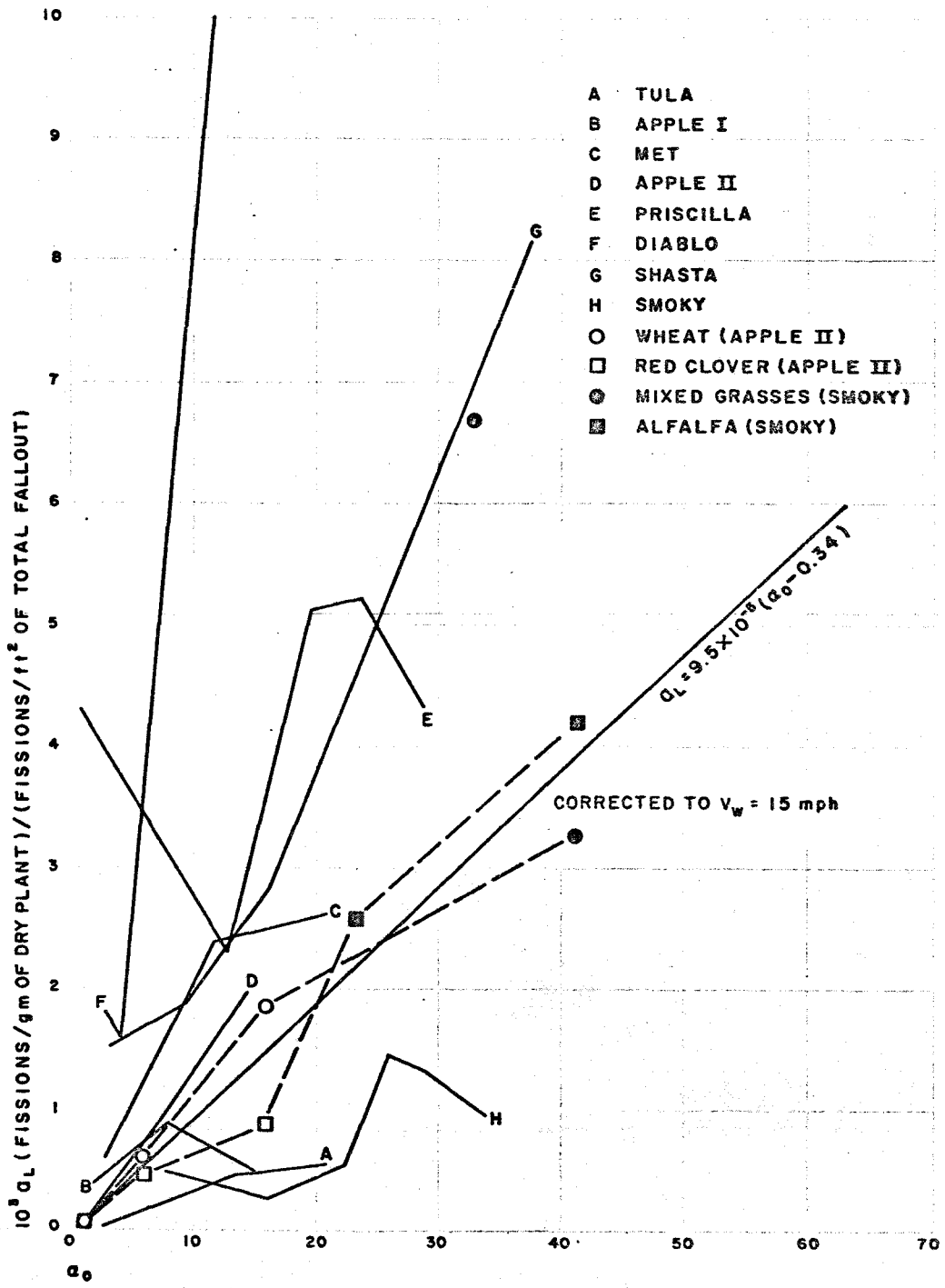

If it is assumed that the surface densities of the clover and wheat foliage in the flats used on Apple II detonation were higher than the average for such crops, then a range of values of w_L may be suggested. These are:

Red Clover	:	w_L = 5 to 25 gm. dry plant/ft^2 of soil surface
Wheat	:	w_L = 10 to 40 gm. dry plant/ft^2 of soil surface
Alfalfa	:	w_L = 10 to 30 gm. dry plant/ft^2 of soil surface
Mixed Grasses	:	w_L = 5 to 25 gm. dry plant/ft^2 of soil surface

Wide variations in w_L from these ranges might occur in various sections of the country.

The fraction of the total fallout that is retained on foliage can be estimated from the product $a_L w_L$. Thus, for a w_L value of 20, the fraction retained is $1.9 \times 10^{-3} (\alpha_o - 0.34)$. In Table 6.8, the value of α_o at the 1 r/hr at 1 hr contour farthest downwind from ground zero is 26.1; at this location, $a_L w_L$ is then 0.049, or about 5 percent, and the calculated value of $r_\alpha(1)$ is 0.77. Hence, from Eq. 6.57, the value of $FC_r(1)$, is 1.6×10^{11} (fissions on foliage/ft^2 of soil area)/(r/hr at 1 hr).

Estimates of the median size (or size-range) of particles retained on foliage may be made if the variation with α_o of the median diameter of the particles in the deposited fallout is known. In Figure 6.7 the values of the median diameters of the fallout lodged on foliage, taken from Table 2.15, are plotted as a function of α_o. For these data, the median diameter of the fallout particles on the foliage increases with α_o; thus, the median diameter of the retained fallout increases as the median diameter of the deposited fallout decreases.

Clearly this trend in the median diameter of the retained particles with α_o could not continue indefinitely since at some point, when the diameters of the deposited fallout particles become very small, all the particles could be retained by the foliage. To illustrate this aspect, calculated values of the median diameter (d_m) for the deposited fallout are also plotted as a function of α_o in Figure 6.7. Extrapolation the linear representation of the data for d_m of the foliage-retained particles as a function of α_o to the curve for d_m of the deposited fallout gives a maximum value of about 57 microns.

The various functional representations of the foliage contamination factor contour ratio, as derived from the data of Romney and coworkers[6], are based on information obtained from nuclear detonations of tower and balloon-mounted devices. However, in the treatment of that data the emphasis was placed on the particular mathematical functions that could be used in making estimates of internal hazard from fallout produced by land-surface detonations.

Figure 6.7
VARIATION OF THE MEDIAN PARTICLE DIAMETER OF FALLOUT ON FOLIAGE WITH α_0 OF THE DEPOSITED FALLOUT

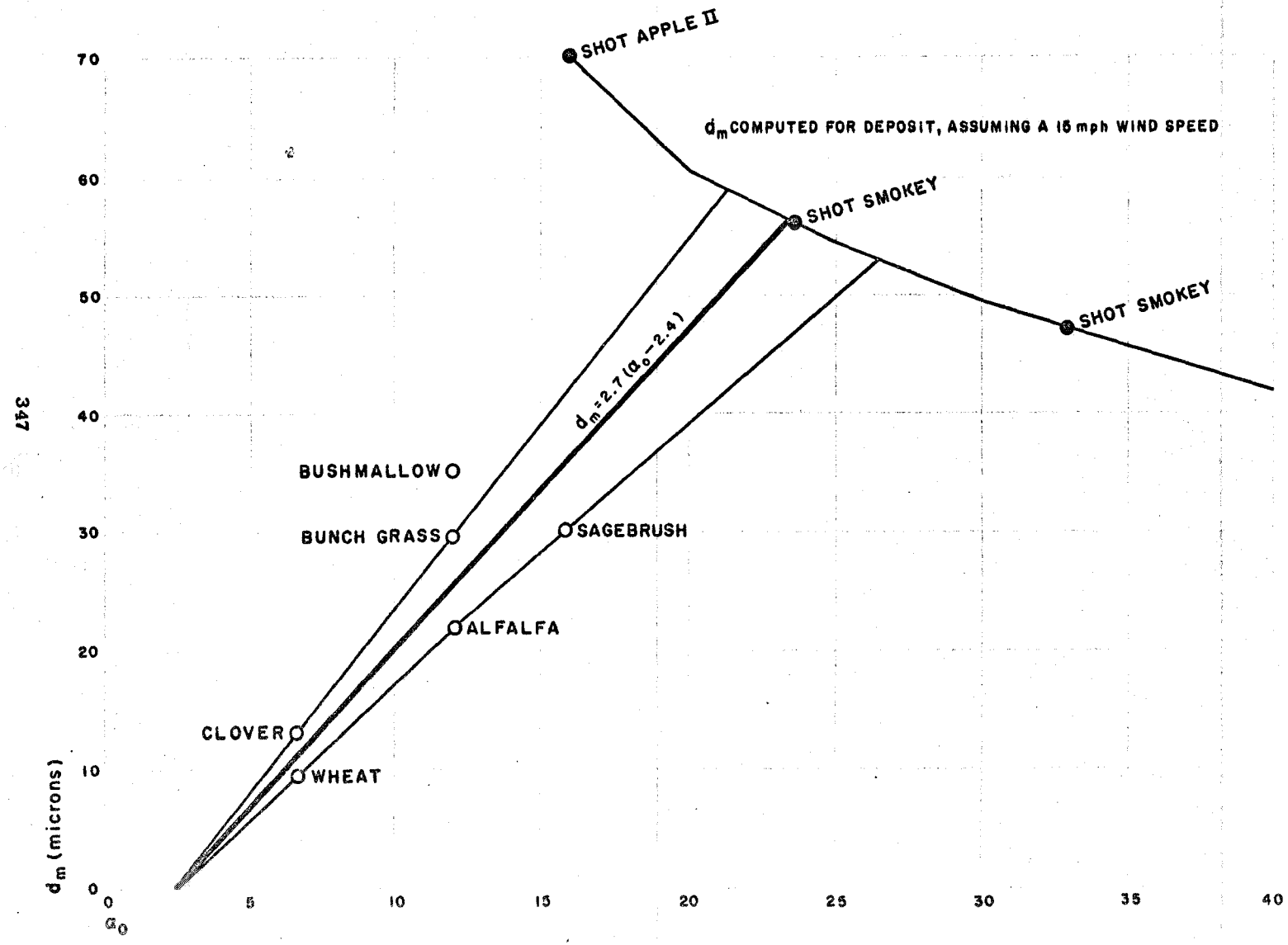

This application should be valid for any condition of detonation since the same physical phenomena must be involved in particle retention by foliage irrespective of the source of the depositing particles. When more data become available, the proposed representations of the processes can be altered to be either more specific for different types of foliage or otherwise more complicated depending on the observed variations in the data.

CHAPTER 6 REFERENCES

1. Bolles, R.C., and N.E. Ballou, Calculated Abundances of U-235 Fission Products, USNRDL-456, 1956.

2. Miller, C.F., and P. Loeb, Ionization Rate and Photon Pulse Decay of Fission Products From the Slow Neutron Fission of U-235, USNRDL-TR-247, 1958.

3. Strope, W.E., Evaluation of Countermeasure System Components and Operational Procedures, Operation Plumbbob WT-1464, 1958.

4. Miller, C.F., Analysis of Fallout Data, I. The Jangle "S" and "U" Shot Fallout Patterns, USNRDL-TR-220, Del. 1959.

5. Morgan, K.Z., et al., Report of ICRP Committee II on Permissible Dose For Internal Radiation (1959), Health Physics, Vol. 3 (1960).

6. Romney, E.M., R.G. Lindberg, H.A. Hawthorne, B.G. Bystrom, and K.H. Larson, Health Physics (to be published).